

# LACUSTRINE RIFT BASIN EVOLUTION AND ORBITAL PACING OF JURASSIC TROPICAL CLIMATE: A COMPARISON WITH THE QUATERNARY MEDITERRANEAN SAPROPEL RECORD

A Field Trip for the International Ocean Discovery Program (IODP)  
Forum Meeting September 14-15, Palisades New York

Paul E. Olsen<sup>1</sup> & Angela Douglass<sup>2</sup>  
September 13, 2022



Stop 4: Cut in the middle and upper Early Jurassic East Berlin Formation (Hartford Rift Basin, CT) showing profound mostly precession-related cyclicity. Entrance ramp to Route 9 from Route 15, East Berlin, CT.

ISBN: 978-0-942081-36-7

<sup>1</sup> Lamont-Doherty Earth Observatory of Columbia University, Palisades, NY 10968.  
(polsen@LDEO.columbia.edu).

<sup>2</sup> Geosciences, Wellesley College, 106 Central Street, Wellesley, MA 02481.



## **ABSTRACT**

This field will visit the Hartford Rift Basin of Connecticut and Massachusetts, one of many continental rifts that formed in a vast extensional zone during 40 million years of the Triassic and Jurassic. This preceded the fragmentation of the supercontinent of Pangea and formation of the earliest Atlantic ocean crust. Filled with more than 6 km of continental strata spanning at least 14 million years, the Hartford Rift Basin is famous for its cyclical, orbitally-paced lacustrine strata that initiated with the flood basalts of the Central Atlantic Magmatic Province (“CAMP,” which may or may not be related to the oldest Atlantic seafloor), and the end Triassic Mass Extinction (“ETE,” which was causally related to the CAMP).

The overriding themes of the field trip are the evolution of the central Atlantic passive margin, orbital pacing of strata recording tropical climate variations (with time control from U-Pb dates), and volcanic winters as the cause of the ETE on land.

We will examine exposures of the fluvial rocks that began the known infill of the basin, the spectacular initial CAMP pillow lavas, the remarkable orbitally-paced Jurassic age strata interbedded with the CAMP flows, amazing little mega-eruption ashes that do not change thickness for hundreds of kilometers (plausibly associated with volcanic winters), one the world’s largest exposure of dinosaur footprints dating from half a million years after the ETE (preserved in the regressive phases of one of the lake cycles), and continuous cores of related lake sediments from the Newark Basin.

A major focus will be specific comparisons between the Quaternary Mediterranean sapropel record, thought to record tropical African monsoonal climate, and these Pangean tropical lakes that when examined with the same timeseries techniques have strikingly similar spectral patterns. While perhaps unsurprisingly dominated by climatic precession al pacing, there is more than a whiff of obliquity, and that, by conventional wisdom, should not be there, in either case. The inconvenient reality of the obliquity pacing in these two tropical but otherwise radically different depositional, greenhouse gas, and tectonic settings calls out for some overriding Earth system processes translating insolation to climate, as opposed to specific rivers, currents, and other temporally- and geographically-specific explanations. Whatever these processes are, they were shared between these two systems separated by 200 Myr, producing records that look rather alike, and we still do not understand them.

## CONTEXT

This field trip is designed around a series of four vignettes, our field trip stops (Figures. 1-5), based on localities in southern Connecticut part of the Hartford Basin component of the Connecticut Valley Basin. While it is quite normal to discount one's surroundings as mundane, deep scientific exploration of virtually anything can reveal deep insights that transcend the provincial and parochial. That is the case with the geology of the Hartford Rift (Figs. 2-5).

Formed during Triassic-Jurassic the sedimentary and igneous rocks of the basin preserve a record of rifting of Pangea and events occurring during the rise to ecological dominance of dinosaurs, with implications for topics as diverse as mass extinction and solar system dynamics.

### East African Rifts



### Central Atlantic Margin Rifts

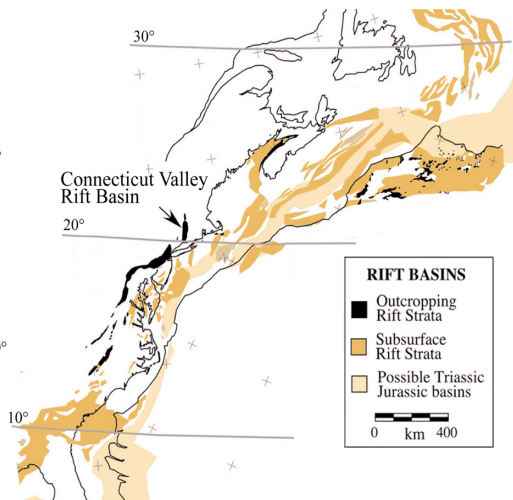


**Figure 2:** Present East African rift system compared to that of Eastern North American and African parts of the Early Mesozoic rift system. From (1).

bisecting Pangea from the present Arctic Ocean through the Gulf of Mexico to the present Pacific Ocean. One of these rift valleys is preserved today as the Connecticut Rift Valley Basin, close to the center of the entire rift system (Figs. 2-3). The Connecticut Valley Rift Basin subsided and accumulated sediments from the surrounding highlands at least from the Late Triassic around 215 to 195 million years ago in the Early Jurassic. During this time the crust in the rift valley slowly

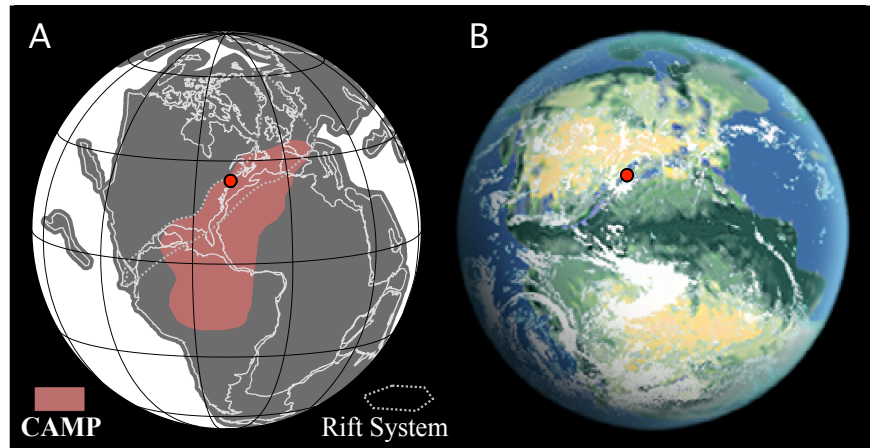


**Figure 1:** Earth at 202 Ma (red dot locates Connecticut Valley Rift Basin); A, outlines of the present continents, the CAMP, and rift system; B, interpretive image showing wet (green) and dry (yellow) areas From (1).

### *The Great Triassic-Jurassic Rift System*

After more than 100 million years of continental assembly, the resulting supercontinent of Pangea (Figure 1), was beginning a long period of extension forming a multitude of rift basins. The initial stages of Pangean disassembly were well underway during the early part the Age of Dinosaurs, the Triassic Period (253-202 million years ago). This early continental rifting produced innumerable faults and their attending rift valleys accommodated the extension, extending over ten thousand kilometres, bi-

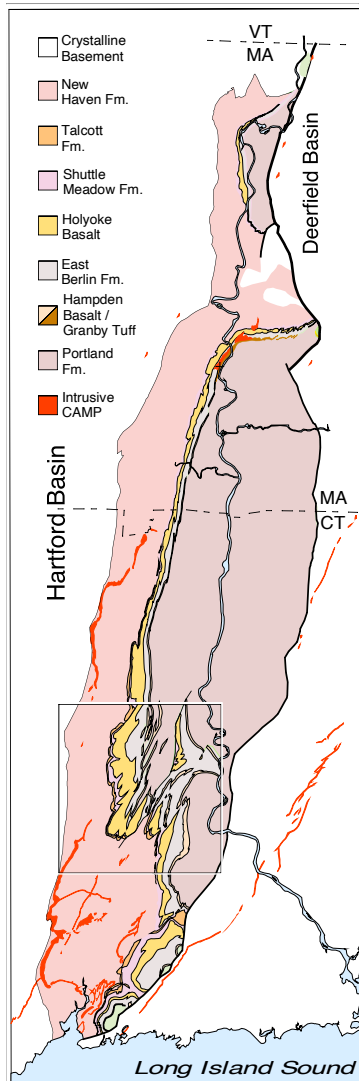


**Figure 3:** Geologic map of the Connecticut Valley Basin. See Figure 5 for key to units. Modified from (1).

dropped asymmetrically along its east side along its west-dipping eastern border fault forming a half graben (Figs. 3, 5, 6), while all the time sediment was pouring in from the surrounding highlands keeping the valley floor nearly flat. During this time more than 6 km of sedimentary and volcanic rocks were deposited in the basin and these are divided into eight formations in the large southern sub-basin of the Connecticut Valley Rift Basin, the Hartford Basin (Figs. 3, 5). These formations are, from the bottom up (Figure 5): the New Haven Formation (**Stop 1**), an overwhelmingly red and tan fluvial unit with some minor lacustrine and eolian strata near the top; the Talcott Formation, a basaltic lava flow formation that often exhibits pillows, breccias, and coarse pyroclastics (**Stop 2**); the Shuttle Meadow Formation famous for its fossil fish; the East Berlin Formation (**Stop 3**), red, gray, and black lacustrine sequences, famous for the very abundant dinosaur footprints with sequences comprising extraordinarily obvious orbitally-paced cycles, similar to those of the Late Triassic Passaic Formation (**Stop 3**), overlain by the Hampden Basalt (**Stop 4**), the uppermost basalt flow formation; and the Portland Formation that is the thickest formation in the basin with a lower red, gray, and black largely lacustrine portion and an upper entirely red fluvial portion. The subsidence of the basin ceased at about the time rifting culminated between North America and Africa with the formation of the first ocean crust between the two continents and the birth of the Atlantic Ocean, although the exact timing of the latter remains murky. Since that time, the rift basin fill has been uplifting and eroding, supplying sediments to the continental shelf.

### The Triassic-Jurassic Greenhouse World

From its inception to its demise, the Connecticut Rift Valley drifted north from about 12° to 21° North Latitude, along with the rest of central Pangea. Thus, this rift valley was in the tropics, drifting northward though its history from more typically humid to more arid climates.

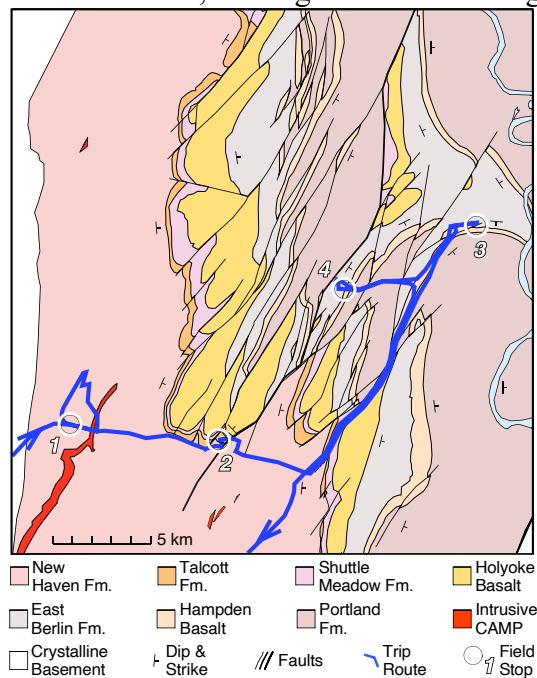


**Figure 4:** Geologic map of field trip area. Location is inset in Figure 3. Modified from (1).

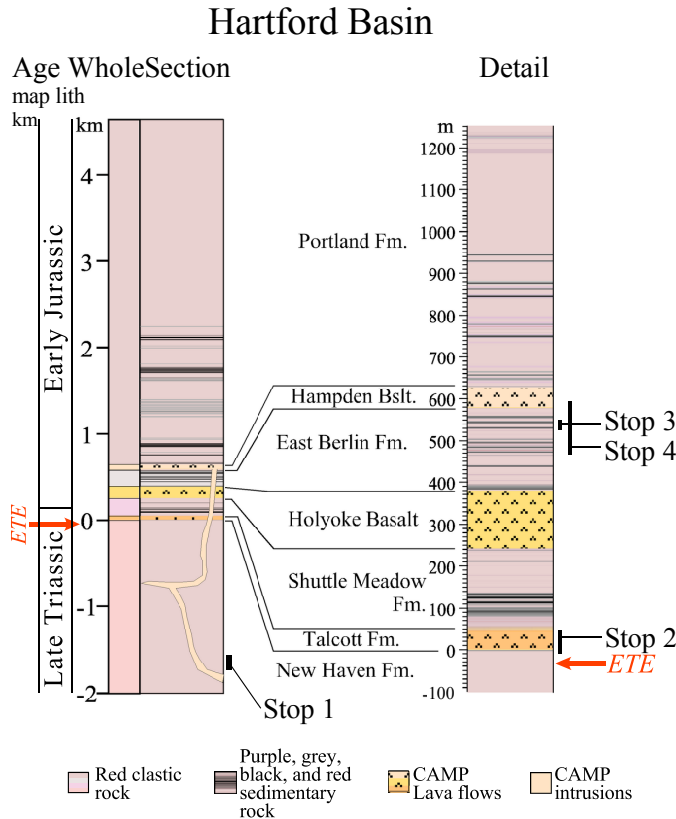


**Figure 6:** The Hartford Subbasin part of the Connecticut Valley Rift Basin showing basic units and field stops. Modified from (1, 8).

located in what were the semi-arid and arid belts of the Triassic where red beds were deposited, drifting to temperate regions later. Overall, because the polar regions today comprise the largest deserts in the world, given that they were covered by vegetation in the Triassic, everything else being equal, the Triassic would be seem to be more “humid” on average than today’s climate,

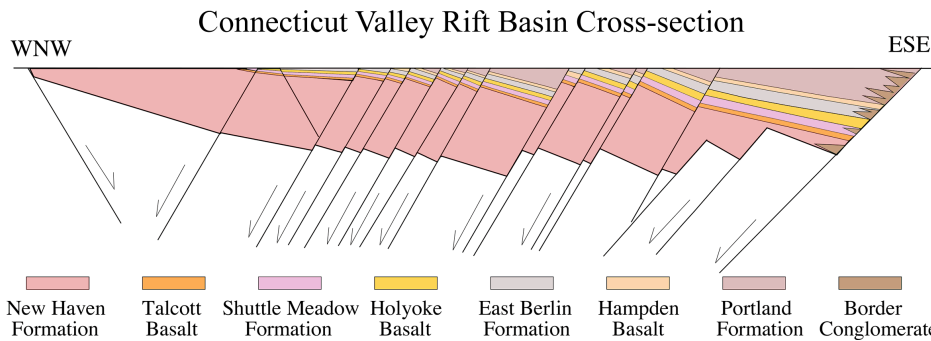


**Figure 5:** Diagrammatic cross section of the central Hartford Subbasin of the Connecticut Valley Rift Basin. From (1).

(Figure 1). While there may have been other contributing factors, the leading hypothesis is that the Earth was in a “Greenhouse” state because of very high atmospheric CO<sub>2</sub>, compared to today. That very high pCO<sub>2</sub>, (~1000 to ~6000 ppm as opposed to the present’s 415 ppm) was normal for this time period is indicated by geochemical and biological proxies (soil carbonate (2-4) and plant leaf stomata (5)) (Figure 7). That does not mean there were not freezing temperatures in some areas. Evidence of freezing winter temperatures takes the form of what appears to be lake-ice-rafted debris in the high Pangean latitudes (>70°N) of at least present northwest China (6) – but without evidence of glaciers or ice caps. The forests of the high northern latitudes also had abundant deciduous relatively large-leaved conifers (7), consistent with a cool winter climate, but nowhere near as cold as today.

The humid tropical regions seem to have spanned about the same latitudes as today, as is also true for the arid belts (Figure 8). Parenthetically, the common characterization of the Triassic being a time of great aridity is largely a function of the early and mid-20<sup>th</sup> century centers of Euro-American geological research accidentally having been located in what were the semi-arid and arid belts of the Triassic where red beds were deposited, drifting to temperate regions later. Although it is worth keeping in mind that area of the Earth north of 60° or south of -60° constitute only 13% the total surface of the globe.

The Triassic-Early Jurassic climate pattern with freezing temperature at high latitudes, which were

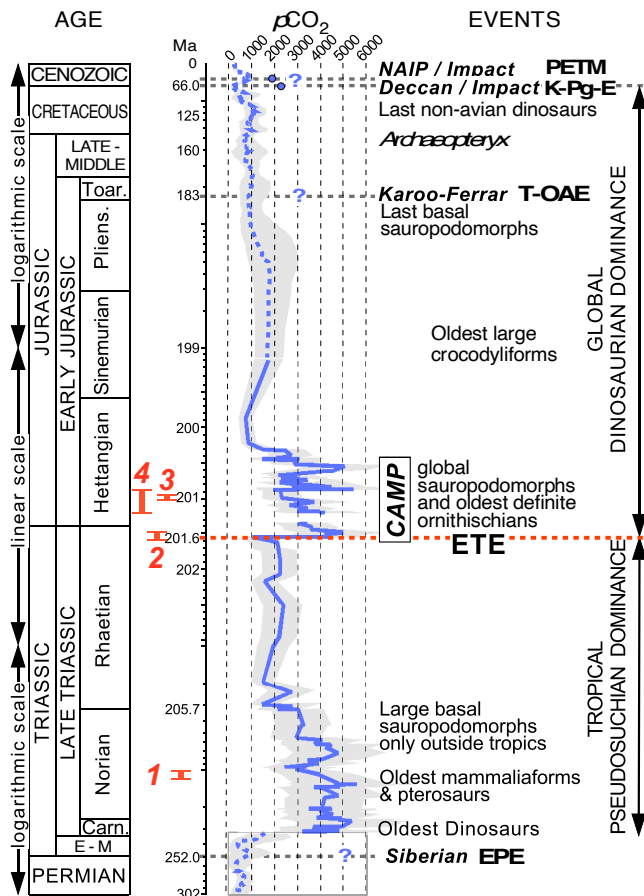


**Figure 7:**  $p\text{CO}_2$  and mass extinction and the field stops in red. NAIP, North Atlantic Igneous Province; PETM, Paleocene-Eocene thermal maximum; K-Pg, Cretaceous-Paleogene boundary; T-OAE, Toarcian anoxic event; ETE, end-Triassic extinction; EPE, end Permian end Permian extinction. Inference of impact at PETM from (6, 15, 16).

restricted to the preserved fill of the Connecticut Valley Rift Basin itself (**Stops 1 and 4**), where they comprise the Talcott Formation, the Holyoke Basalt, and the Hampden Basalt (Figure 5), although the intrusions that fed them extend far beyond. These flood basalt lavas are resistant to erosion and underlie landmarks familiar to Valley residents such as the Hanging Hills of Meriden (**Stop 1**), Lamentation, Totoket and Talcott mountains, and Mt. Tom and Mt. Holyoke. Parts of the plumbing that fed those lavas also make prominent hills, such as East Rock, West Rock, and Sleeping Giant.

also heavily vegetated, is a pattern that is probably key to the evolution and ultimate ecological expansion of dinosaurs as explored below.

### **CAMP: Earth's Largest Volcanic Province**

For nearly all of its Triassic history, the rifting of most of central Pangea was singularly devoid of volcanism, with the exception of a small set of granitic intrusions in New Hampshire and Maine [(9-11) and references therein] and another set of volcanic and igneous units in Italy [e.g., (12)]. That quiet came to an abrupt and terrific end with the emplacement of the gigantic Central Atlanctic Magmatic Province or CAMP. Remnants of intrusions and lavas of this mostly basaltic province are spread over a Pangean area of about 11 million square kilometres (Figure 1), which for reference is about 1/3 the area of the moon.

CAMP rocks are found in northern France, Germany, the Iberian Peninsula, Morocco, most of the rest of the Maghreb, West Africa, Eastern and Southern North America, Guyana, Surinam, French Guiana, Brazil, Bolivia, and possibly Sicily. In places that are not as deeply eroded as exposed basins of Eastern North America, such as Morocco and on the continental shelves, flood basalt lavas of the CAMP are very widespread, while in exposed rocks of New England, the lavas are

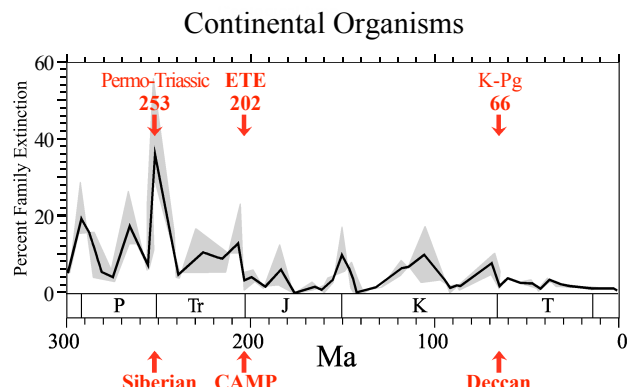


**Figure 8:** Extinction rate for continental organisms with positions of the 3 major mass extinctions and associated flood basalt provinces (from ref. 1, 13, 14).

The oldest CAMP intrusions and flood basalt flows date from about 202 million years ago, more than 30 million years after the rift system formed and at least 13 million years after the Connecticut Valley Rift Basin began accumulating sediment. The eruptions and intrusions seem to have ended very quickly as well, within 2 million years. This is very different than rifting areas today, such as in East Africa, where volcanism has been dribbling on for ~30 million years.

However, the abrupt, massive but short-lived CAMP, began at the onset of the end-Triassic mass extinction or ETE (Figure 8) and is the most parsimonious explanation for that event. The ETE is one of the “Big-Five” mass extinctions of the last 600 million years and one of the three largest of the last 300 million years, including the famous Cretaceous-Tertiary (K-T, or more properly the K-Pg) mass extinction at 66 million years ago that witnessed the end of the non-avian dinosaurs and the end-Permian extinction that is known as the “Great-dying” (13) (Figure 8). These later two mass extinctions are also associated with flood basalts with a similar abrupt, massive but short-lived history, specifically the giant Siberian Traps overlapping the end-Permian event and the Deccan Traps overlapping with the K-Pg event. Of course the latter is famously even more precisely synchronous with a giant bolide impact at Chicxulub, and which more simply explains the observed pattern of K-Pg extinctions.

CAMP volcanism is also conspicuous for its lack of airfall ashes. However, two remarkable examples are present in a well-developed deep-water lacustrine unit in the East Berlin Formation and its equivalents (Figure 9). These are called the Pompton Ashes and they are known from 10 sites in the Newark and Hartford Basins over a distance of 200 km. They would seem to be the results of super-eruptions based on their lack of change of thickness over the distance they are known. They provide evidence of sulfur aerosols that plausibly resulted in intense volcanic winters.

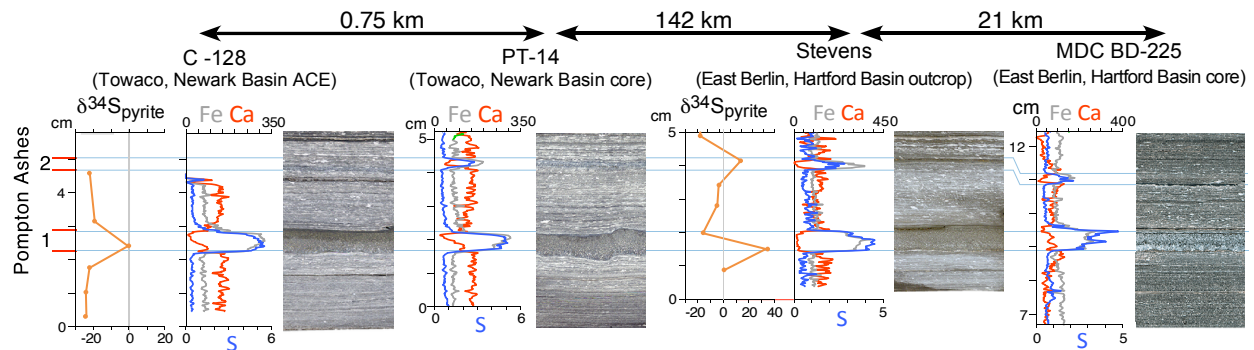


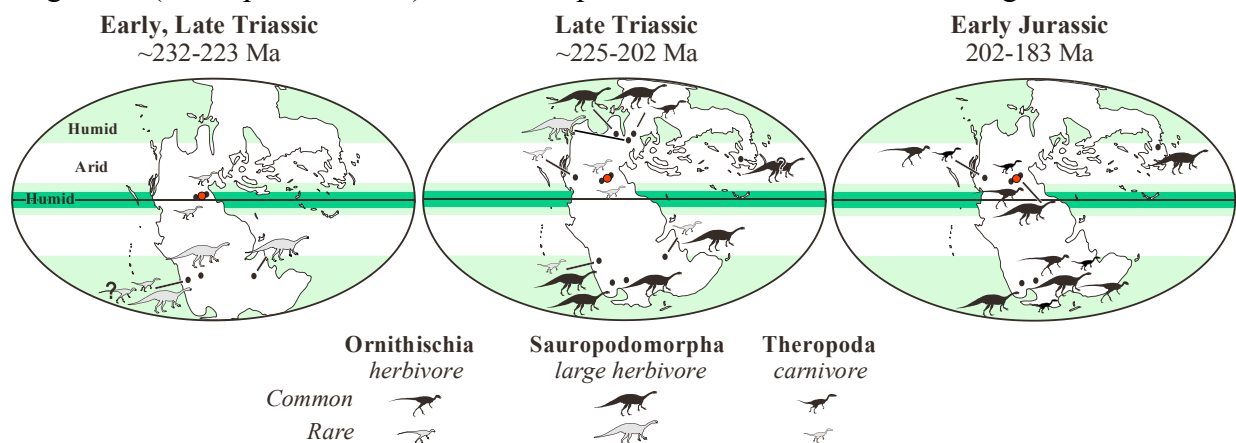
**Figure 9:** Sections of key Pompton Ashes 1 & 2 across a 164 km transect with XRF chemical data (Itrax: counts  $10^3/\text{sec}$ ) showing S (pyrite) spikes in ashes (17-19) with  $\delta^{34}\text{S}_{\text{pyrite}}$  data (6, 16, 20).

**Pompton Ashes.** The Pompton Ashes are the only airfall tuffs known in the entire 11 million  $\text{km}^2$  CAMP area. In addition to assuring precise and accurate correlation between cycles in the East Berlin and Towaco Formations in the Hartford and Newark Basins, they provide critical proof of concept of the occurrence of explosive sulfate-rich CAMP eruptions and their effects on environmental proxies as elaborated below. The Pompton Ashes are comprised of the lower, main 5-mm-thick Pompton Ash and an upper 1-mm-thick “2<sup>nd</sup> ash” at 10 localities in the Newark and Hartford Basins (Figure 9). They are graded, composed of sharply euhedral plagioclase laths in an originally glass matrix, with fine-grained feathery feldspars, carbonate, and sub-mm volcanic spherules at its base (18, 21). The thinner ash is similar to the thicker, but with smaller grain size. The ashes stand out in  $\mu$ -XRF scans (Figure 9) as excursions in S and Fe, inversely correlated to Ca, undoubtedly tracking pyrite of post-depositional origin. They show no discernible thickness change over 200

km, and profiles of the ashes from slabs 142 km apart are similar at the sub-mm-scale, making them reliable marker beds. The Pompton Ashes were fortuitously deposited during the highstand of a chemically stratified lake, the undisturbed and highly visible ash layers occurring within microlaminated, fossil-fish-bearing, dark mudstone with no bioturbation. If deposited in shallower water units of the East Berlin and Towaco Formations, similar ashes would likely have been reworked and weathered and be cryptotephra (22-24).

### ***Protofeathers, the End-Triassic, and Jurassic rise of Dinosaurian Ecological Dominance***

The Triassic witnessed the evolutionary origin of all of the major groups of land vertebrates alive today, specifically modern amphibians, turtles, lizards, crocodylians, dinosaurs (alive today as birds), and mammals (more properly “protomammals”) (Figure 8). But there were also “holdovers” from the Paleozoic such as giant temnospondyl “amphibians” and parareptiles. There were others that arose and went extinct in the Triassic, such as the great evolutionary radiation of the pseudosuchians, and a whole suite of diverse and bizarre, swimming, gliding, digging, and climbing forms, as well as a few groups that survived the Triassic but died out later in the Cretaceous or at the K-Pg boundary such as the flying-dinosaur-relatives the pterosaurs. A major evolutionary innovation within some of these groups (mammals, dinosaurs plus pterosaurs) was an insulatory integument (fur or protofeathers) that had implications for their survival through the ETE and K-



Pg mass extinctions (6).

**Figure 10:** Early Late Triassic to earliest Jurassic (~232 – 200 Myr) Pangea showing the distribution of known dinosaurs (from 1, 6, 16). Red cross is location of Connecticut Valley Rift Basin.

***Delayed Dinosaurian Dominance.*** Given the fact that dinosaurs arose in the Triassic and were around by 232 million years ago, it has come as a rather large surprise that they not only appear first at high (southern) latitudes, but all herbivorous forms stay restricted to the high latitudes of both hemispheres for the rest of the Triassic, until the ETE, 30 million years later (16, 25, 26) (Figure 10). Where herbivorous dinosaurs are found in the Late Triassic in the higher latitudes, they are very abundant, often the most abundant of all land animals found. In contrast the Triassic tropical regions of Pangea have not produced a single bone or verifiable footprint of an herbivorous dinosaur, including areas famous for abundant skeletal remains such as the Chinle Formation of the Western United States. Instead, the tropics were dominated by large pseudosuchian reptiles, that included the lineage that gave rise to modern crocodylians, but far more diverse. Included are the crocodile-like phytosaurs (independently evolved), herbivorous forms some of which were dramatically convergent on dinosaurs, giant carnivorous top-predators, and a myriad of small

forms (Figure 7). Some small dinosaur relatives are present, that did include some relatively common herbivorous as well as carnivorous forms, but the only true dinosaurs present were relatively small carnivorous forms that with the exception of one or two localities are very rare. This surprising bi-polar distribution of Triassic dinosaurs, coupled with the new climatic information about the cool high latitudes provides clues to both survival of dinosaurs through the ETE as well as their spectacular Jurassic ecological ascent.

**Protofeathers.** After John Ostrom’s 1970s revival of Thomas Henry Huxley’s late 1860’s argument that birds are the direct descendants of dinosaurs (27), providing Darwin with the first clear “missing link” predicted by “*The Origin of Species by means of Natural Selection*”, several young firebrands, including Robert T. Bakker proposed that dinosaurs were metabolically more like birds or mammals than like crocodiles or lizards. Bakker (28) and Greg Paul (29) implicitly revived another late 19<sup>th</sup> century idea and suggested that feathers may have evolved not for flight but rather for insulation and were already present in non-avian dinosaurs, notably the carnivorous theropods, like *Velociraptor*. By 1986 they were drawing them feathered. This concept was not popular with ornithologists (30)! What should have been a massive boost to the idea was the earlier (1971) (31) discovery in Kazakhstan lake sediments of a Jurassic pterosaur covered in filaments, clearly a form of insulation. [There was a much earlier (1831!) notice of such filaments (32, 33), but it was largely ignored.] Because pterosaurs are close relatives of dinosaurs, but not dinosaurs themselves, the simplest hypothesis possible is that these insulatory filaments were a kind of “protofeather” and that the common ancestor of pterosaurs (6, 34, 35) and dinosaurs and all of its descendants would have had protofeathers (Figure 11). Of course in large forms they could have been lost or reduced,

not being needed for insulation because of “thermal inertia” (36), just like Asian elephant adults are nearly hairless but their babies are quite hirsute. Instead, until recently, most of the community poo-pooed the idea, preferring instead to get wrapped up in progressively more contorted arguments to keep the feathers of birds unique. However, discoveries in lake sediments in China and Siberia of Jurassic and Cretaceous age, rather like those at **Stop 4**, have demonstrated without any doubt that filamentous integuments, that is “protofeathers” were widespread not only in theropod dinosaurs (37), including large ones (38), but also in small plant-eating ornithischian dinosaurs (35, 39).

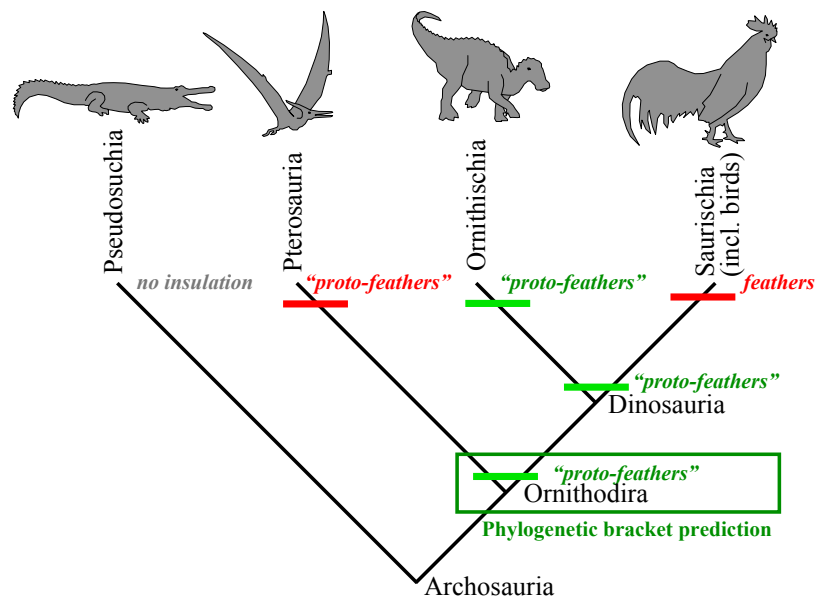


**Figure 11:** Phylogenetic relationships of major groups within the Archosauria showing the predictions of the phylogenetic bracket for insulation by feathers and “proto-feathers”. Observations made before 1996 are shown in red. Green are predictions of the phylogenetic bracket approach corroborated by discoveries after 1999. This assumes that the “proto-feathers” (pycnofibers) of pterosaurs are homologous with feathers in birds. This is controversial but consistent with recent discoveries (e.g., 6). From (1).

Further, these fossils also show that these protofeathers evolved in animals that were never capable of any sort of flight (37) and that filamentous protofeathers were only later co-opted by natural selection for flight. This argument ends up being critical to the origin of dinosaurs, the distribution of Triassic dinosaurs, and the survival of dinosaurs through the ETE and their ecological ascent.

***Dinosaurs are Fundamentally Cool-Climate-Adapted.*** Compared to most of the low latitudes, the vegetated high latitudes plausibly provided a predictable and large food source for herbivores. However, the new Chinese data of lake-ice-rafted debris, suggest that these regions were not just cool but had freezing winter temperatures (6, 40). There is absolutely no evidence that the uninsulated herbivorous, or for that matter carnivorous pseudosuchians, so diverse and abundant in the tropics, could survive in such a climate. However, insulated dinosaurs with high metabolisms and their close relatives could survive. The dinosaurian herbivores common to the higher latitudes are the so-called “prosauropods”, or more correctly basal sauropodomorphs, such as *Plateosaurus* that were the largest herbivores of their time. None have actually been found as yet with protofeathers, and none have been found in lake deposits likely to preserve them. However, the simplest hypothesis is that they had protofeathers, as did their ancestors (Figure 11). None have yet been found in association with evidence for seasonal ice in the coal-bearing areas either, such as northwestern China, largely for lack of looking. However that gives us an opportunity to make a specific prediction and that is that they will be found in these coal-bearing high-latitude strata, and when they are, the terrestrial assemblages will lack pseudosuchians.

But why did the low latitudes lack herbivorous dinosaurs for 30 million years after they evolved? A reasonable explanation is that the very high CO<sub>2</sub> of most of the Late Triassic (Figure 7) exaggerated tropical climatic extremes, as is suggested by models of the effects of current rising anthropogenic CO<sub>2</sub> (41). The seasonal and longer term climatic cycles would be exaggerated, and along with higher temperatures, there would plausibly be a high frequency of fire and plant resources would be unpredictable. Evidence for this is provided by stable carbon isotopic, spore and pollen evidence, and fossil charcoal (16). There is strong evidence for the correlation between high atmospheric CO<sub>2</sub> and exaggerated climate extremes in the Triassic-Jurassic lake sediments of the giant Pangean Rift system, most notably from here in the Connecticut Valley Rift Basin (**Stop 4**) and the Newark Rift Basin, the next major basin to the south (Figure 2). The lower metabolic requirements of the herbivorous pseudosuchians suited them well for unpredictable resources, and that may have made dinosaurian herbivory non-competitive in the tropics, until pseudosuchians were nearly wiped out during the ETE.

The conclusion from this is that the common ancestor of dinosaurs and their close relatives the pterosaurs, was insulated, had high metabolic requirements, and was fundamentally adapted to cooler, high latitude climatic regimes, not the hot tropics.

***The ETE.*** Eruption of the CAMP lavas and emplacement of associated intrusions would be expected to have pumped enormous amounts of CO<sub>2</sub> (and possibly methane) and sulphur aerosols into the atmosphere, with dramatically contrasting environmental effects (42). Rising CO<sub>2</sub> would produce global warming that would last for tens to hundreds of thousands of years, as well as transient, if extreme, ocean acidification (if the rates of eruption were high enough). In contrast, the sulphur aerosols would cause global dimming and lead to volcanic winters (43) that would fade quickly – 3 to 5 years – after each eruption ceased. The pattern of extinctions of marine invertebrates is consistent with ocean acidification from the abrupt absorption of CO<sub>2</sub> but the patterns of

both animal and plant extinctions are more consistent with extreme volcanic winters, as opposed to the direct effects of global warming (6).

CO<sub>2</sub> proxy data from soil carbonates from the Hartford (**Stops 1 and 4**) and Newark rift basins in sediments around the CAMP flood basalt lavas (Figure 7), as well as from leaf stomata from north of the CAMP area [paleo-mid-latitudes (5, 44)], show that CO<sub>2</sub> doubled to tripled in three to four pulses of CAMP eruptions taking hundreds of thousands of years to drop down to background levels after each pulse (3, 4). The CO<sub>2</sub> levels in the 2000 to 6000 ppm after each pulse of CAMP eruption were not that different than the background levels of most of the Late Triassic (2), but CO<sub>2</sub> had been dropping for 5 million years before the CAMP, and then rose precipitously (Figure 7). Plausibly each doubling may have taken only hundreds of years, rather like what is happening now.

Each CO<sub>2</sub> doubling would be predicted to increase temperatures globally by an average of about 3° - 5° per doubling assuming the consensus climate sensitivity estimated by the Intergovernmental Panel on Climate Change [IPCC (41)]. This sensitivity is theoretically independent of the starting value, but its value is nearly entirely model dependent and not well tested by data for present CO<sub>2</sub> concentrations, not to mention starting at 2000 ppm or so. The actual temperature changes could be larger or smaller or could depend on unknown feedbacks that could themselves vary with initial concentrations. Nonetheless, it is hard to see how an increase in the 3° range could be important except in marginal areas and especially hard to see how it could effect land communities already adapted to heat and extremes. This is notably true when migration into higher latitudes or up mountains were ecological options, especially when such high CO<sub>2</sub> values persisted for 10s of millions of years during most of the Late Triassic (Figure 7) and the same organisms were thriving.

On the other hand, the sulphur aerosol-driven volcanic winters that may have been severe enough to freeze the tropics, even for a few days, could have had the effect of wiping out all large non-insulated land animals, especially large pseudosuchians and a large variety of warm-adapted plants. In contrast to the options available from a warming, victims of tropical cold had nowhere to go – everywhere else was worse. In contrast, insulated dinosaurs and pterosaurs were already “pre-adapted” to volcanic winters as were the plants in high latitudes. It is noteworthy that the high latitude floral changes were minor compared to what happened in the tropics and some groups such as the deciduous conifers went through the ETE without any change (7).

Thus, the pattern of extinction on land seems more in line with volcanic winters than global warming. While proxy development of sulphur aerosols in sediments is still in its infancy, the volcanic winter hypothesis does make the prediction that there should be evidence for freezing in the Pangean tropics. This evidence could be in the form of ice-rafted debris in lake strata, or impressions of ice crystals in the kinds of sedimentary strata that would otherwise have footprints. Another form of evidence would be the effects on lacustrine sulfur reducing bacteria by fertilization of lakes by sulfur aerosols during and shortly after eruptions, Such fertilizations should shift pyrite sulfur isotopes  $\delta^{34}\text{S}_{\text{pyrite}}$  in the gray and black units towards negative values.

It is worth remembering, however, that the amount of time represented by the volcanic winters may be very short, and that the strata had to have been deposited during a time when major CAMP eruptions were happening somewhere else – in other words the evidence won't be recorded in the lava layers themselves. In the Hartford Sub-basin of the Connecticut Valley Rift there are at least five sedimentary intervals in which to look: 1) the ETE interval itself in sedimentary strata below the Talcott Basalt Formation; 2) the lower Shuttle Meadow Formation; 3) the middle Shuttle Meadow Formation; 4) the basal East Berlin Formation; and 5) the lower Park River Member of

the Portland Formation. Only the basal East Berlin Formation, however has strata in which specific lava flows were unambiguously erupting during sedimentation. Finding such evidence will be tricky, not only because evidence is likely to occupy vanishingly small proportion of the thickness of the strata, but also because there are other mechanisms to raft in coarse debris into a lake than ice, notably root balls of trees, bushes and other plants, or floating algal (cyanobacterial) mats all of which are already known from Connecticut Valley lake strata. Even evaporate crystal impressions might be confused with those of ice. The sulfur isotopes, especially if associated with evidence of cooling from clumped isotopes may be the best bet for finding evidence of volcanic winters.

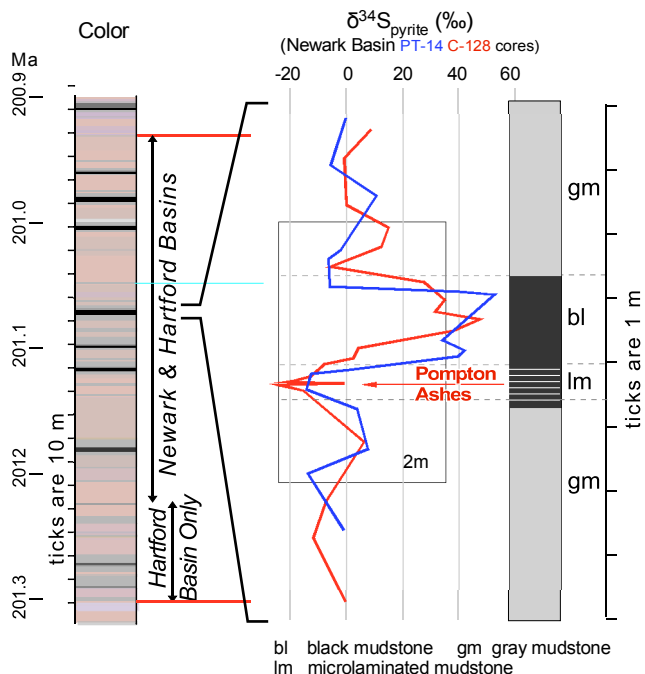


**Figure 12:** East Berlin Formation (left) with data from Newark Basin lacustrine cycle correlative to the Westfield Bed (**Stop 4**) of the East Berlin (right). Data from Stueeken et al. (20). See Figure 9 for detail of core C-128 around Pompton Ashes.

Support is provided by the data of Stueeken et al. (20) from two cores of a single precession-related lacustrine cycle in the Towaco Fm of the Newark Basin, and outcrops of the coeval Westfield Bed of the East Berlin Fm in the Hartford Basin (Figures 9, 12, 14) (**Stop 4**). Average background  $\delta^{34}\text{S}_{\text{pyrite}}$  hovers around 0‰ in gray, shallow-lake strata that bracket the black highstand bed. Most of the latter is characterized by a dramatic positive excursion in  $\delta^{34}\text{S}_{\text{pyrite}}$  to between +40‰ to +60‰, interpreted as a result of closed-system microbial sulfate reduction in a progressively  $^{34}\text{S}$ -enriched reservoir. As this lake filled and reached its outlet during its early, hydrologically-open phase,  $\delta^{34}\text{S}_{\text{pyrite}}$  in the basal microlaminated, fish-bearing basal layers of the highstand bed would be expected to remain around ~0‰. Instead,  $\delta^{34}\text{S}_{\text{pyrite}}$  became more depleted than anywhere else in the cycle (-20‰), suggesting an input of sulfate into the lake. This same negative excursion is also seen at two outcrops of the East Berlin Fm of the Hartford Basin (Figures 9, 12, 14). As this is the exact interval hosting the Pompton Ashes

at all sites, we think this negative excursion is most simply interpreted as a consequence of direct inputs of volcanic aerosols from eruptions augmented by drainage of airfall sulfate from the surrounding watershed diffusing into porewaters.  $\delta^{34}\text{S}_{\text{pyrite}}$  values have been used to infer volcanic aerosol input from the Siberian Trap eruptions into marine strata at the close of the Permian (67). Unlike the interval around the Pompton Ashes, however, these end-Permian excursions in  $\delta^{34}\text{S}_{\text{pyrite}}$  cannot be related to specific volcanic eruptive events. Examination of the basal East Berlin Formation would prove fruitful because that interval was deposited simultaneously with the eruptions of the know CAMP flows in other basins (45), although that would require coring like that proposed at Dinosaur State Park. The prediction is that the basal East Berlin would exhibit very strong negative shift in  $\delta^{34}\text{S}_{\text{pyrite}}$  and cycles with no ashes higher in the East Berlin would only exhibit the strong positive excursions due to reservoir effects. Additional supporting evidence of volcanic sulfur aerosols is  $\text{SO}_2$  acid rain damage of plants at the ETE from the moist mid-latitudes (46, 47).

**Survivors.** Most groups that made it through the ETE, are still extant now. These include the dinosaurs (as birds), crocodylians, turtles, lizards and their relatives the sphenodontians, modern amphibians, and mammals. Also surviving were pterosaurs, some protomammals (such as the tritylodonts and trithelodonts), one other non-crocodylian lineage of pseudosuchians (sphenosuchians), and a very few archaic “amphibians” that did not make it through the K-Pg event. The only non-insulated forms surviving from Triassic continental communities were either forms small enough to burrow or forms that could hibernate in lakes. This pattern is again consistent with survival from volcanic winters. Strikingly, the latitudinal segregation of herbivorous dinosaurs ends at the ETE, and subsequent latest Triassic and Early Jurassic assemblages became remarkably uniform globally and dinosaur size, especially among theropods increased dramatically, marking global ecological ascent of the dinosaurs.

However, compared to the Triassic, the post-ETE assemblages were of remarkably low diversity. This is especially notable in the footprint record in the Connecticut Valley Basin (Figure 13) (Stops 3 and 4). This footprint record is overwhelmingly dominated by small to large carnivorous theropod dinosaur forms - the brontozoids, including *Grallator*, *Anchisauripus*, and the Connecticut State fossil, *Eubrontes* (8). Also fairly abundant were tracks of small protosuchian crocodyli-forms (*Batrachopus*), much less common footprints of herbivorous small ornithischian dinosaurs (*Anomoepus*), some medium sized to fairly large herbivorous “prosauropod dinosaurs” (*Otozoum*), and exceptionally rare lizard- and mammal-like forms (*Rhynchosauroides* and *Ameghinichnus*, respectively). This low diversity at high taxonomic levels might mask much higher species-level diversity that we have as yet no clear way to gauge. What is known is that these post-ETE assemblages are much lower in diversity at high taxonomic levels than those that existed before the mass-extinction.

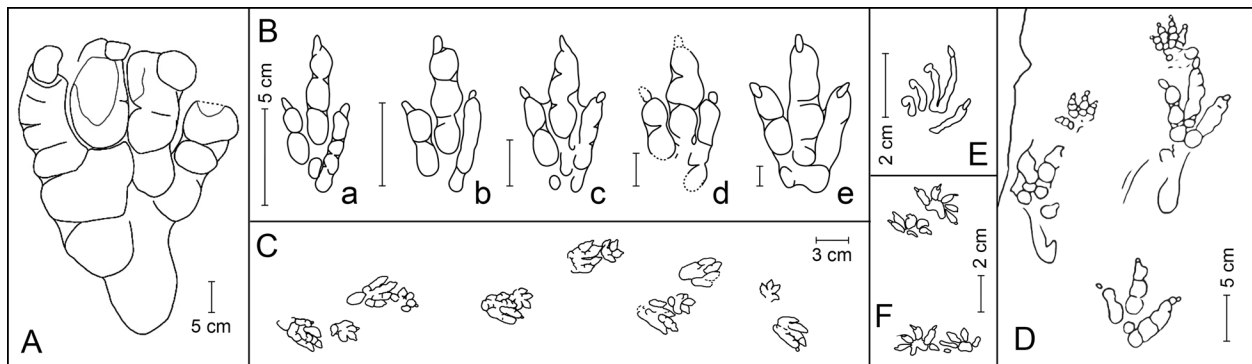


**Figure 13:** Post ETE footprints of the Connecticut Valley. A. *Otozoum moodii* a herbivorous “prosauropod”. B, Brontozoid tracks made by carnivorous theropod dinosaurs; a, *Grallator parallelus*; b, *Grallator parallelus*; c, *Anchisauripus sillimani*; d, *Anchisauripus tuberosus*; e, *Eubrontes giganteus* (Scale is 5 cm for all). C, *Batrachopus deweyii* made by a crocodyliiform; D, *Anomoepus intermedius* (= *A. scambus*) made by a small ornithischian dinosaur; E, *Rhynchosauroides* sp., made by a lizard-like forms; F, *Ameghinichnus* sp. made by a “proto-mammal” or mammal. These are drawings of actual specimens, all from ref. (1, 8).

The apparent striking numerical dominance of carnivores that seems to be a violation of the basic trophic or Eltonian ecological pyramid may be real. The base of the food chain may have been largely aquatic as we will discuss at **Stop 3 and 4**, and the carnivorous dinosaurs may have primarily subsisted on fish and other carnivores that ate fish (48). Track assemblages from younger Middle and Late Jurassic deposits have much more abundant herbivores suggesting the

recovery to a more “normal” looking terrestrial community with more herbivores than carnivores.

**Cyclical Climate, a Time Scale, and the Chaotic Evolution of the Solar System.**

The lakes that deposited most of the sediments in the Connecticut Rift Basin rose and fell due to climate changes that were in synchrony with celestial mechanical cycles driven by the Moon and planets (Figure 14). These lake level cycles controlled the depositional environments in the basin and hence the distribution of different sediments appearing as a vertical patterning of sedimentary cycles and also controlled the distribution of fossil. The climate changes themselves, fluctuating from humid to hyper-arid, obviously had a major role in the kinds and distribution of organisms that lived in the region.

**Origin of the Cyclicity.** The daily and seasonal cycles of environmental change, light vs. dark, summer vs. winter, are caused by the changes in the distribution and intensity of sunlight driven by the rotation of the Earth about its axis and combined effects of the tilt of the axis and the orbit of the Earth around the sun (Figure 15), which play out differently depending largely, but not exclusively on latitude. On larger timescales, the orientation of the Earth’s axis and the shape and orientation of the Earth’s orbit also change, and this alters the daily and seasonal cycles as part of climate change. These changes in the orientation of the Earth’s axis are largely driven by gravitational forces of the Moon and Sun on the equatorial bulge of the Earth and the changes in the Earth’s orbit and are also driven by effects of all the other bodies in the Solar System. The rotation of all of those bodies around the Sun result in complex gravitational rhythms passed on as rhythms and resonances in the combined axial and orbital features of the Earth, which then affect climate.

The gravitational rhythms combine like many musical notes to produce a kind of celestial music to which the planets dance, and the results are not quite periodic, but rather are quasisperiodic changes in the distribution and intensity of sunlight per unit area, called insolation, that are also expressed variably with latitude. The complex insolation rhythms play out over tens of thousands of years to millions of years and are the familiar Milankovitch cycles, after the Serbian meteorologist (Milutin Milankovic) who produced a quantitative explanation how these orbital changes could have paced the ice ages of the last two million years of Earth History. While these Milankovich cycles in insolation are quite subtle, especially compared with the daily and seasonal cycles, the Earth

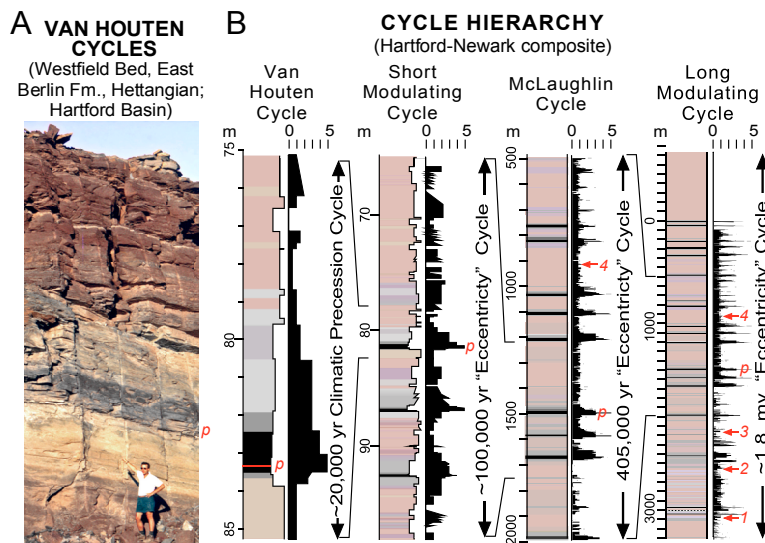


**Figure 14:** Orbitally-paced sedimentary cycles in Hartford and Newark Basins. A, 20 kyr precession-paced cycle at East Berlin, CT (Westfield Bed). B, Cycle hierarchy of relevant latest Triassic-Early Jurassic age Newark-Hartford composite (47). Basalt flow formations: **1**, Talcott & Orange Mt; **2**, Holyoke & lower Preakness; **3**, top of upper Preakness; **4**, Hampden & Hook Mt. **p**, Pompton Ashes.

System apparently non-linearly amplifies their effects to the point that they are major features of climate. These climate cycles unfold, of course, within the context of changing  $p\text{CO}_2$  boundary conditions that determine if climatic cycles are glacial ages, or wet-dry alternations.

While various astronomical theories of climate change appeared in the mid-19<sup>th</sup> century, nearly at the same time that it was realized there were repeated Ice Ages, and a quantitative theory linking celestial mechanics with the Ice Ages was developed by Milankovic in the 1920s, it was not until the famous 1976 “Pacemaker” paper of Hays, Imbrie, and Shackelton (52) that it became widely accepted that the Ice Ages and climate changes of other times, were paced by changes in the Earth’s orbit and axis. The key insights involved applying mathematical techniques of signal processing (Fourier time series analysis) to long sedimentary, deep-sea core records. It quickly became obvious that other aspects of the Earth’s climate system were paced by Milankovitch cycles, including tropical wet-dry cycles.

The most important Milankovitch cycles are quasiperiodic at periods of around 21, 41, 100, and 405 thousand years (kyr) and 1.2 and 2.4 million years (Myr). In fact, the cycles of 21, 41, 100 kyr are actually averages of several cycles with similar periods. The 21, 100, and 405 kyr and 2.4 Myr cycles are related to a wobble of the Earth’s axis (precession), modulated by the shape and orientation of the Earth’s orbit (eccentricity), while the 41 kyr and 1.2 Myr cycles are related to the angle of the Earth’s axis relative to the plane of the Earth’s orbit (obliquity), modulated by the rocking of the plane of the Earth’s orbit (inclination). All of these cycles appear in Earth’s climate record (50, 53-55).

The geometry of the parameters of the Solar System from which orbital frequencies can be derived are shown in Figure 15. The secular fundamental frequencies are the precession of perihelion of planetary orbits ( $g$  frequencies) and precession of the node of the plane of planetary orbits ( $s$  frequencies). Linear differences of the  $g$  frequencies give us the frequencies of the eccentricity of the Earth’s orbit and those of the  $s$  frequencies give us the frequencies of the inclination of the Earth’s orbit. Linear sums of the  $g$  frequencies with the frequency  $p$  (axial precession = 1/25.7 kyr) give us the frequencies of climatic precession, and likewise the sums of the  $s$  frequencies and  $p$  give us the obliquity

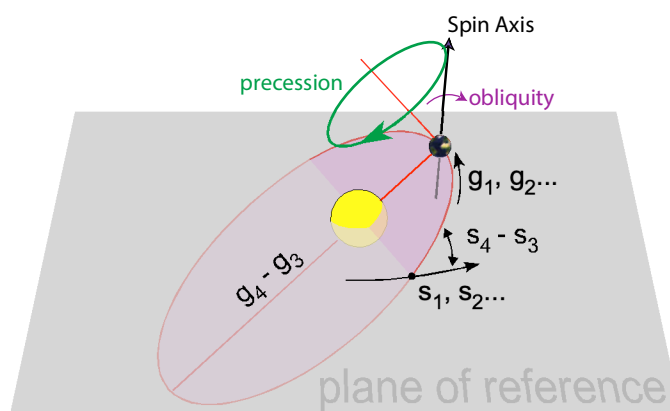


**Figure 15:** Basic geometric elements of variations in the Earth’s orbit and the Earth’s axis contributing to Milankovitch cycles. Modified from refs (13, 48, 49). The  $g_1, g_2, \dots$  are frequencies of precession of perihelion for each planet, 1 being Mercury, 2, Venus, etc. The  $s_1, s_2, \dots$  are frequencies of precession of the node of intersection of the Earth’s orbital plane with the reference frame (essentially Jupiter’s) for each planet. Linear difference combinations of the  $g$ ’s are the frequencies of eccentricity, e.g.,  $g_2 - g_5 = 1/405$  kyr, the “long”-eccentricity, metronomic Jupiter-Venus cycle and  $g_4 - g_3 = 1/2.4$  Myr, today’s value for the highly chaotic Mars-Earth cycle. Likewise, Linear difference combinations of the  $s$ ’s are the frequencies of inclination, e.g.,  $s_3 - s_6 = 1/173$  kyr metronomic inclination cycles. The axial precession frequency,  $p = 1/25.7$  kyr added to the  $g$ ’s give the climatic precession frequencies, e.g.,  $p + g_5 = 1/23.7$  kyr. The obliquity frequencies are likewise  $p$  added to the  $s$ ’s, e.g.,  $p + s_3 = 1/41$  kyr. Difference combinations between climatic precession frequencies and likewise with the obliquity frequencies, e.g.,  $(p + g_5) - (p + g_4) = g_5 - g_4 = 1/95.0$  kyr, one of the short eccentricity cycles.

frequencies. The  $g$  and  $s$  difference combinations are independent of  $p$  which varies with the Earth-Moon distance — being shorter in the past when the Moon was closer. However, the  $g$  and  $s$  frequencies do drift because of gravitational resonances and are chaotic over long time periods, with the most massive planets being the most stable and the least massive ones, the least stable, and that is reflected in the combinations. Thus,  $g_2-g_5 = 1/405$  kyr is metronomic over billions of years, as is  $s_3-s_6 = 1/173$  kyr, while  $g_3-g_2 = 1/2.4$  Myr today is very unstable and had the frequency  $1/1.8$  in the Late Triassic as is observed in the Newark Rift Basin (49).

**Cycles in the Triassic and Jurassic.** Milankovitch cycles also affected climate, presumably since the origin of the lithosphere-hydrosphere-atmosphere system and of course in the Triassic and Jurassic in the Hartford Rift Basin. The repetitive sedimentary patterns, that are the lacustrine sedimentary cycles, are a major feature of the Shuttle Meadow, East Berlin, and lower Portland formations (Figure 14). Without large outcrops, exposures, or cores, however, these cycles can be

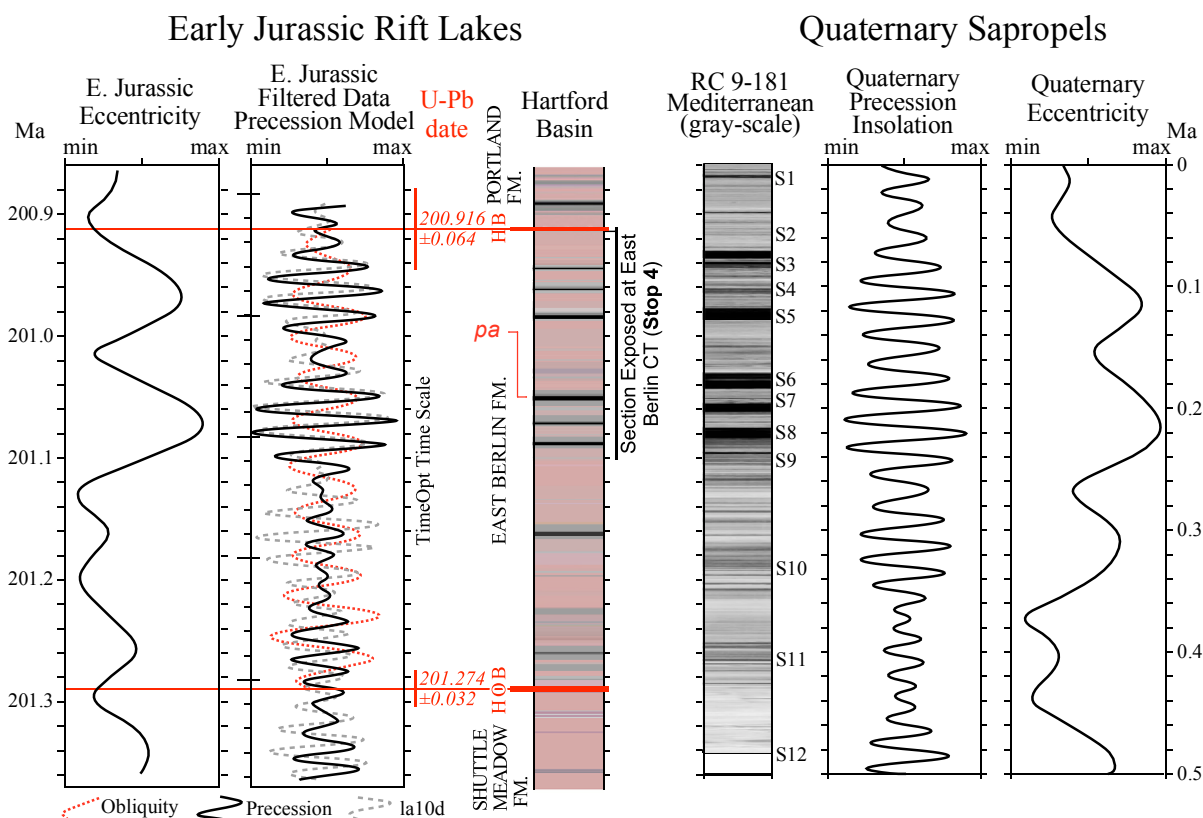


**Figure 16:** Comparison of the Early Jurassic East Berlin Formation cyclical lacustrine section with the Quaternary Mediterranean sapropel sequence in core RC9-181 collected in 1965. Both are thought to record tropical monsoon variations in precipitation. East Berlin section based on MDC cores and section at East Berlin, CT (Stop 4) (47). Gray scale image of RC9-181 from (54) slightly modified to account for compaction. To derive the precession and obliquity curves for the East Berlin Formation, climate-sensitive lacustrine facies “depth ranks” were assigned a constant accumulation rate based on TimeOpt implemented in Acycle (55, 56) analysis which were then filtered at the 201 Ma frequencies for climatic precession and obliquity. The Early Jurassic eccentricity curve is a Hilbert transform [Amplitude Modulation (56)] of the precession curve from the East Berlin data. For RC9-181, the precession and eccentricity curves are from the La2004 solution (57) and for the East Berlin Formation from (56, 58). U-Pb dates are from (59). *pa* is position of Pompton Ashes; **HB** is position of Hampden Basalt; **HOB**, is position of Holyoke Basalt.

hard to see, because the cycles are so thick (10 to 20 m) and the rock exposures tend to be so small. As with the sunlight changes that drove the environmental cycles, the rock cycles are not precisely repetitive, and instead there are cycles within cycles, within cycles and we will see these cycles at one of the largest exposures we will visit (**Stop 4**) in the East Berlin Formation of Early Jurassic age (Figure 16).

The mechanism thought to produce the environmental cyclicity seen in these lake sediments is relatively simple in outline and the same as that now governing the long-term behavior of climate in much of the tropics. The mechanism is like that of the tropical, African Monsoon system, in which a zone of rain tracks the zone of maximum summer heating that in turn, tracks the dates that the sun is overhead. The magnitude of the rain varies with the magnitude of the insolation and therefore the lakes behave like rain gauges. The average state of the lakes in the Connecticut Valley Rift Basin was very shallow and often dry, so even though the insolation changes in Milankovitch cycles are sinusoidal, the Connecticut Valley Rift the obvious cyclicity reflects primarily the positive deviations from the mean – the lake can't get any shallower than dry.

What we see in the sedimentary sequence are cycles consisting of a shallower water lake deposit, deepening upward (transgressive), followed by a lake high-stand deposit formed when the lake was at its maximum depth (and insolation was at a maximum), followed by a shallowing water deposit (regressive), and then a generally thicker interval of very shallow water deposits (low stand) that in some cases have fossil soil sequences (paleosols). These are the primary cycles mostly caused by the ~20 kyr climatic precession cycles and they are modulated by eccentricity cycles with the effect of causing the expression of high-stand deposits to vary from black, to gray, to purple or even red, while the shallowest water sediments tend to be red all the time. This produces a bundling of cycles with black strata, separated from bundles of cycles without black strata. The very deepest of the lakes were so deep, perhaps hundreds of meters, that the lower part of the water column was devoid of oxygen and microlaminated mudstones were produced, often preserving complete fish. The shallowest water units, in contrast, tend to be more massive and have abundant desiccation cracks, root impressions and soil carbonate nodules, and reptile footprints. The cycles, thus, also determine the fossil content. The soil carbonate nodules provide a proxy in their carbon isotopic composition of atmospheric CO<sub>2</sub>. Field **Stop 4** in the East Berlin Formation shows this cyclicity beautifully.

These cycles, because they are hypothesized to have tracked celestial mechanical cycles, allow the measurement of time in the sedimentary strata that have them. In the 1980s, and 1990s, Olsen et al. (62-64) used them to estimate the amount of time between CAMP flows and thus measure the duration of the part of the CAMP event preserved in the Connecticut Valley and the Newark rift basins, coming up with a value of about 610 kyr for the duration of all three lava flow formations. Only within the last few years have radiometric dating techniques, specifically U-Pb method become precise enough to test this hypothesis. In 2013 (61), the flows were dated using zircon U-Pb CA-ID-TIMS with a precession of 60 kyr or less and showed that the predictions of the Milankovitch hypothesis for these lacustrine strata were correct. The modern geological time scale for the Late Triassic and early part of the Early Jurassic is based on these lake cycles, pinned in time by the radiometric dates from the CAMP lavas (61). The dates for the various field stops on this trip are based on this astronomically calibrated time scale.

***Solar System Chaos.*** Because the Solar System is a complex, moving array of bodies gravitationally interacting, it is a dynamical system, potentially subject to chaotic behaviour. Its long-term behaviour can only be described by numerical (as opposed to analytical) solutions, the validity of

which is measured in 10s of millions of years. In fact, numerical solutions of the Solar System show chaotic behaviour over timescales greater than about 60 million years (50). The effects within the last few hundred million years are measurable only for the cycles with periods greater than the 405 kyr cycle. Those longer cycles act like interferometers varying in frequency by the differences of frequencies of the  $\sim 20$  kyr precession and  $\sim 40$  kyr obliquity cycles. This is predicted to show up in the very long eccentricity cycle that presently has a period of 2.4 Myr years and the inclination cycle of 1.2 Myr, when these cycles are examined over hundreds of millions of years. Those two cycles are manifestations of the interference of gravitational cycles caused by Earth and Mars, that themselves cannot be measured, but the periods of those cycles are predicted to vary in period by more than a million years over the last 200 million years - and that can be measured. Furthermore Earth and Mars are locked in a resonance that can theoretically flip the ratios of the eccentricity and inclination cycles from 2:1 to 1:1. In contrast the other cycles are predicted not to vary much at all, with the 405 kyr cycle (due to Jupiter and Venus) being extremely stable, the  $\sim 100$  kyr cycles varying practically immeasurably (65), and the present 41 Kyr and 21 Kyr cycles decreasing in period back in time due the recession of the moon. Thus, the Early Jurassic periods were closer to 35 kyr and 19 kyr respectively, because the moon was closer, which as mentioned we can see at **Stop 4**. These measured Late Triassic and Early Jurassic cycle periods as well as their phases strongly corroborate that the Solar System is chaotic, but they also do not exactly match any of the current astronomical solutions for that chaos, which ultimately they must [although La10d is quite close (45, 50)]. The reason for these discrepancies could be as arcane as measurement error in the present positions masses and velocities of Solar System bodies or as potentially far reaching as an incomplete theory of gravity. Whatever their origin, the empirical geological record can be the ultimate arbiter of the astronomical solutions.

***Obliquity in the Tropics?*** The expression of orbitally forced changes in insolation play itself out primarily in latitude. The traditional interpretation is that obliquity cycles should have virtually no effect in the tropics, while gaining in importance in higher latitudes. However, it is the Earth System that translates insolation to climate and we still don't understand how exactly that works. The code words are that the Earth System responds non-linearly to the orbital forcing, which means it is not simple. For example, the mid-Pleistocene transition is a change from predominantly  $\sim 40$  kyr pacing to predominantly  $\sim 100$  kyr pacing as seen in ocean records reflecting ice volume. The astronomical forcing has not changed, rather it is something in the Earth System that has changed. Because the transition occurs as  $p\text{CO}_2$  was dropping over that time period it is natural to think that  $p\text{CO}_2$  has something to do with it — but what? The problem is a vexing one and had had a plethora of explanations [e.g., (66-69)], There is a similar problem for the effects of obliquity.

The overall section of the East Berlin Formation, much like the much longer record in the Newark basin, seems pretty obviously paced by the linked precession and eccentricity (Figure 16A,B). However we have tight time control afforded by zircon, CA-ID-TIMS U-Pb geochronology that date the Hampden Basalt above and the Holyoke Basalt below [by way of the Newark Basin (49, 61)]. Using the accumulation rate derived from these ages, or using a statistical method termed TimeOpt, which matches a precession-eccentricity pattern to the data, the results show that the expected periods of climatic precession are precisely recorded (Figure 17A). However, unexpectedly, there is an expression of the obliquity band as well. Both sets of frequencies are shifted the right amount to match the insolation model which incorporates the recession of the Moon.

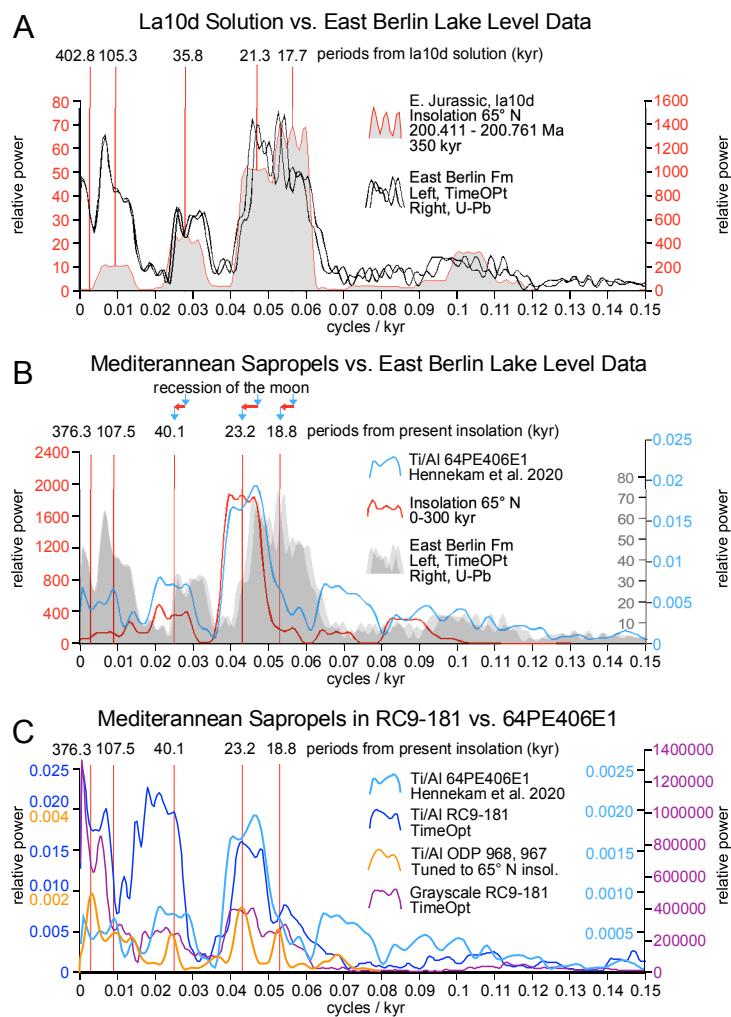


**Figure 17:** Comparison of MTM (multi taper method) power spectra of data and models for climate sensitive sedimentary facies for the Early Jurassic East Berlin Formation and for the Quaternary sedimentary record of tropical monsoonal variations in the Mediterranean Sea core RC9-181, both recording tropical monsoon variations. Note the unexpected obliquity frequencies in both the Early Jurassic lacustrine sequence and the Quaternary marine section. Data from (47, 54, 55, 57, 58, 70), implemented and analyzed in Acycle (56).

**Comparison to Sapropel Records in the Mediterranean.** When PEO was in a graduate student in the late 1970s and 80s, he was struck by the similarity of pattern between the black shales of the Newark and Hartford Basins and the sapropels in the classic Mediterranean RC9-181 core as described by Martine Rossignol-Strick in 1983 and 1985 (73, 74). A piston core, RC9-181 was collected in 1965 from 2286 m of water by the Lamont vessel the Robert D. Conrad on the Mediterranean Ridge halfway between Crete and the border between Libya and Egypt — a portion of this core will be on display **Stop 3**.

The Hartford Basin was in the tropics at the time at about  $21^\circ$  N (70). An insolation model for that latitude, or any latitude in the tropics, has essentially no power in the obliquity band, no matter what age. It might be excused as a coincidence, however, obliquity power has also been reported for the Triassic Passaic Formation of the Newark Basin (71) and in that case passes stringent internal tests (72) (although in that case the studied portion of the record was deposited during the drop in  $p\text{CO}_2$  and related drop in expression of precession-eccentricity cyclicity characteristic of the younger Late Triassic — Rhaetian — prior to the ETE). So somehow, the Earth System was responding to the obliquity pacing in the tropics. One might be tempted to explain this away by some peculiarities unique to the time, such a continental position and the “Mega-Monsoon”, or ocean currents, or mountains, but the problem is we see the same thing in the record of the African monsoon as recorded in Mediterranean sapropels (see below).

The sedimentary rhythms characteristic of the lacustrine sequences of the Connecticut Valley Rift Basin, thus, not only parse the kinds of fossils preserved, but they also provide a time-scale for the sequence and give us a window into the behaviour of the Solar System and the early Mesozoic Earth System response to orbital forcing.

The Mediterranean is a giant, nearly landlocked, body of water that is a remnant of the Tethys Sea. Inflow or relatively low density Atlantic water through the Straits of Gibraltar and an outflow of more saline water results in a vigorous thermohaline circulation that keeps the bottom of the sea relatively oxygenated. Core RC9-181 consists of intervals of organic carbon poor (0.1–0.2%) light foraminiferal and coccolith ooze, like that being deposited today, alternating with much darker, more clay- and more diatom-rich finely laminated layers that are organic-rich (~1–10%) called sapropels. At least some of these sapropels are microlaminated (Figure 18), resembling East Berlin fish-bearing laminites. Early on it was recognized that the sapropels correlated with times of high insolation at precessional minima (74) (Figure 16).

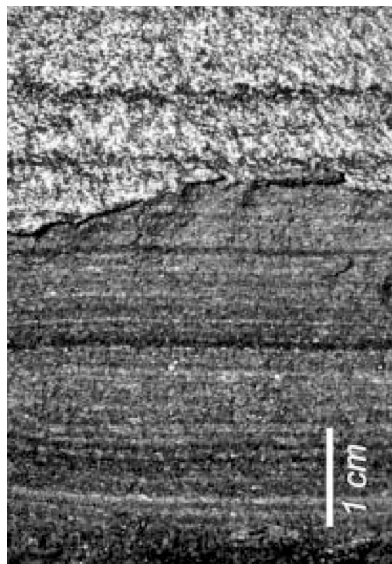


**Figure 18:** Microlaminated diatom-rich sapropel S8 [modified from (79)] revealed by freezing and lifting off scraped out layer of core.

Two, not completely exclusive theories (76), have been used to explain this pattern: 1) enhanced export productivity leading to greater bacterial respiration and reduced bottom water oxygen (77); or 2) disruption of the normal thermohaline water circulation leading to bottom water oxygen depletion (74). Both hypotheses rely on an influx of fresh water due to tropical monsoon precipitation during precessional insolation maxima. A additional influence on sapropel formation involves sea level changes modulating Atlantic Ocean water inflow in the Mediterranean modifying the thermohaline system (78).

Despite the thousands of papers that discuss the hundreds of cores from the Mediterranean Sea, there are very few published time series analyses [e.g., (80, 81)] of Quaternary sapropel sequences from cores, despite the intense efforts and historical importance of spectral analysis to our understanding of paleoclimate. In order to examine the spectral properties of sapropel cyclicity, Douglas et al., (56, 82) examined new grayscale (from archival photographs) and new XRF data from core RC9-181, and published XRF data from core 64PE406E1 (83), and reflectance data from ODP 964 and 966 (84) to see how untuned data or minimally tuned data (not to insolation or a precession solution). The results of the spectral analyses (Figure 16B, C) are completely consistent with the insolation-tuned data of Konijnendijk et al. (80) in showing an important amount of spectral power at the obliquity frequency (1/41 kyr). In order to produce spectra similar to the data using insolation the canonical 65° N at June 21 must be invoked. As recognized by Konijnendijk et al. and others, this presents a problem because the monsoon precipitation response to orbital forcing in the tropics supplying Nile water should show basically no obliquity. The observed strong obliquity component has generally been explained by evoking features of the African and Mediterranean climate system specific to the present geography [e.g., (75, 85, 86)], which certainly might be valid, on the face of it. But, as described above, the same pattern is seen in the Early Jurassic tropical records of lake level and that record was formed in a world about as different from the present day as possible within the last 300 million years.

Thus, it seems more plausible that these climate responses are the consequences of general features of how the Earth System translates orbital forcing to orbital pacing, than coincidental accidents of different geographies producing the same result.

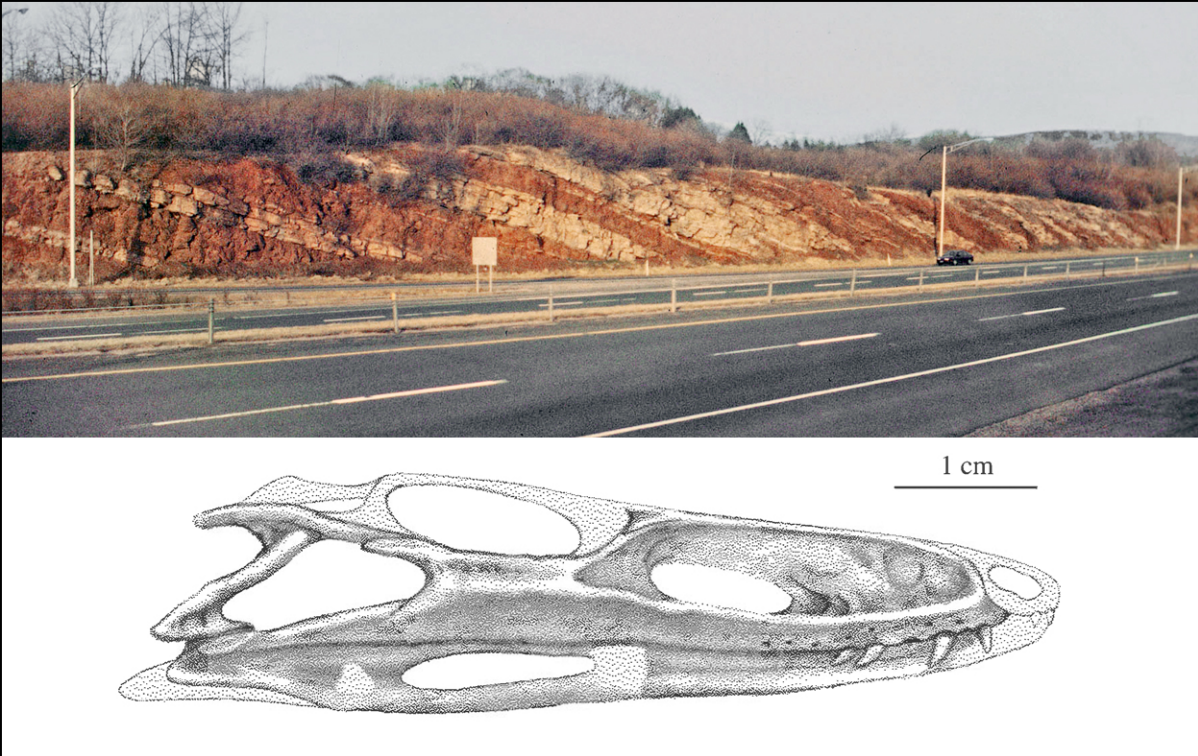


**Figure 19: Stop 1**, New Haven Formation, at Cheshire CT along I 691: above, outcrop as it appeared in 1996; below, skull of *Erpetosuchus* found near left light post (above) (light stipple is reconstructed next to dated caliche that also provided  $p\text{CO}_2$  measurement).

## FIELD TRIP STOPS

### General Plan

The field stops are organised in stratigraphic order, from oldest to youngest, starting in the New Haven Formation and Talcott Basalt Formation, and ending in the Portland Formation and forming more or less a loop in geography (Figures 3, 4). Thus, they also proceed from the time of the ETE into the recovery of that mass extinction.

### Stop 1: Triassic Fluvial Deposits in the Early Hartford Rift

Location: 41.559367°, -72.907017° (Cut along I691, Cheshire, CT)

Units: Lower New Haven Formation

Time: ~212 Ma – middle late Triassic (Norian)

Environments: Fluvial braid rivers and overbank soils

Highlights: Slow subsidence relative to infill, crocodylomorph skull in paleosol, carbonate U-Pb and  $p\text{CO}_2$

Leave vehicle below overpass of Peck Lane, and walk west to location. Stay close to guard rail well off highway. A permit from the CT. Department of Transportation is required to visit this site.

This exposure along Interstate 691 reveals about 130 m of New Haven Formation (Figure 19) dipping about 10° towards the boundary fault of the Hartford basin (Figures 3, 4). The section begins about 650 m above the base of the 2-km-thick formation and consists entirely of deposits of meandering streams and rivers (87). The kinds of deposits seen here are characteristic of the

lower part of the formation in much of the basin. According to McNerney & Hubert (87), this section consists of 22 cycles, each composed of cross-bedded white, gray and buff channel sandstone and gravel and overlying red massive muddy sandstone and mudstone of floodplain origin. They interpret these cycles as being produced by the migration of a meander belt towards and away from the outcrop area. In addition, they recognize four "megacycles" showing an upward increase in amount of time it takes to form the caliche profiles (88). No single climatic type can be assigned to the caliches. Perhaps they formed during the drier phases of the longer climate cycles (? ~100 kyr cycles). The meter scale cycles at this outcrop, for the most part, cannot be traced across the highway and, because they are formed by the lateral migration of rivers and streams, there is no reason to believe they are caused by cyclical climate change. The megacycles of McNerney & Hubert (87), however, might very well be caused by climate change, perhaps the 400 kyr cycle. Our ability to interpret climate change from fluvial sequences is just in its infancy.

Thicker beds of sandy mudstone commonly contain root casts, carbonate nodules, and tubules that form discrete layers. The carbonate layers are interpreted by Hubert et al. (88) as caliche horizons formed on the flood plains. They believe that the caliche profiles are indicators of semi-arid conditions after Gile et al. (89). In any case, the flood plain ecosystem was characterized by very high ecosystem efficiency with virtually every trace of organic matter being respired. That this was due to high consumption as opposed to low productivity is evidenced by the extraordinarily intense bioturbation by the putative arthropod burrow *Scoyenia* and roots that have obliterated virtually all small-scale and even many large-scale sedimentary structures of physical origin such as ripples or mudcracks.

The New Haven Arkose, quite unlike coeval coarse-grained facies in the Culpeper, Gettysburg, and Newark basins, apparently does not grade laterally into lacustrine deposits, and paleocurrent data indicate through-flowing streams. Thus, transgressive-regressive lacustrine cycles are absent from the New Haven Arkose. Nonetheless, if periodic climate change was responsible for the precession-related Van Houten cycles in the contemporary strata from other adjacent basins, then those climate fluctuations must have influenced the Hartford basin as well. Because the duration of the climatic cycles may be similar to the amount of time it takes to form the caliche profiles (88), no single climate type can be assigned to the caliches and associated strata of the New Haven Arkose. It possible the caliches may have formed only during the drier parts of the climatic cycles, or some in between climatic condition.

Direct U-Pb dating of calcite from the soil carbonates of this exposure yields a  $^{238}\text{U}/^{207}\text{Pb}$ - $^{206}\text{Pb}/^{207}\text{Pb}$  isochron age of  $211.9 \pm 2.1$  Ma (90), which makes it coeval with the lacustrine Metlars Member and associated units of the Passaic Formation and the carbonate  $p\text{CO}_2$  estimate for that part of the Passaic is consistent (91). Given this constraint, and an age of about 201.6 for the age of the Talcott Formation (61), the accumulation rate of the succeeding approximately 1350 m of New Haven Formation yields a net average accumulation rate of about 2.6 m/20 kyr which is close to half the average for the contemporaneous Newark basin strata (49). This low accumulation rate supports the hypothesis that accommodation space grew at a lower rate than in the Newark basin and that correspondingly footwall uplift could not keep up with the downcutting of streams and rivers entering from the footwall drainages, and for this reason lacustrine sedimentation did not begin until the major extension pulse of at the onset of CAMP volcanism.

Red mudstone from this exposure has also produced a skull of a small crocodile relative, *Eretosuchus* (Figure 19), in fact the only other skull of this animal outside of Scotland (92, 93).

Participants are advised to keep their eyes open for any other animal remains that might lurk among the mudstones at this location!

## Stop 2: Mega-Eruptions and Mass Extinction

Location: 41.552652, -72.816832 (back parking area of Meriden Target)

Units: New Haven Formation and Talcott Basalt Formation

Time: 201.564 Ma – latest Triassic (late Rhaetian), just after the ETE

Environments: Fluvial to shallow lacustrine and subaqueous flood basalt

Highlights: Oldest CAMP lavas in CT Valley Rift, ETE, pillow basalts, ashes

Leave vehicle and proceed to southwest corner of parking lot. Do not go up to the outcrop; we are here at the discretion of the owners. We will walk north along the west side of the parking lot to the northwest corner of the parking lot traversing parallel to the face of the exposure.

This spectacular exposure reveals nearly the entire thickness of the Talcott Basalt Formation resting on the uppermost few meters of the New Haven Formation (Figure 20). This is the oldest basalt Formation of the CAMP in the Connecticut Valley Rift Basin and lies close to and above the ETE.

***New Haven Formation, the ETE, and Hyaloclastite vs Ashes:*** At the base of the pillowed basalt sequence are red, well-bedded, laterally continuous, internally stratified sandstones and siltstones with graded beds comprised of small *clasts of basalt and highly altered basalt* (Figure 21). These overlie “normal looking” New Haven Formation red beds. Beneath the pillow foresets and associated red beds there is well-bedded red sandstone and mudstone of the New Haven Formation. The basalt and what presumably was basaltic glass is generally altered to a yellow or tan material. All stages of alteration from unquestionable nearly unaltered basaltic material to the tan to yellow clasts seem to be visible. Based solely on macroscopic examination, the lowest beds of the New Haven Formation at this outcrop seem to lack basaltic material.

The basaltic material in the red beds has two simple possible origins. First, is that they could be beds of hyaloclastite shed from the advancing lava flows. Hyaloclastite is a hydrated igneous rock composed of angular, flat fragments 1 mm to a few cm across formed by



**Figure 20:** Pillowed basalt complex of the Talcott Formation. A, Pillow forest overlapping red strata of the New Haven Formation, with graded beds of hyaloclastite; white arrow shows upper surface of foreset. B, Pillow basalt overlain by massive basalt of the feeder flow lobe (*fl*). From (1).

granulation of the lava front due to quenching when lava flows into, or beneath water. They might be mobilized in the water by convection and steam and then settle out as graded beds. Arguing for this is the coarse-grained nature of some of the material and the fact that hyaloclastites are commonly associated with pillowed lavas, often under them. However, similar facies are not associated intimately within the pillow lavas themselves, suggestion that it was not an ongoing process during the entire time that the pillows were being extruded. Although locally deformed by the overlying pillow wedges, these volcanoclastic beds can be traced across this, admittedly limited, exposure of the New Haven Formation indicating that the volcanic material must have been transported a considerable distance to even out their thicknesses. Conversely, while similarly graded volcanoclastic beds have been observed in the uppermost New Haven, about 1 km east at Hubbard Park (41.556086°, -72.825998°), the cm-scale stratigraphy differs, indicating either differences in local depositional patterns, or slight differences in source position.

But, another possible origin is that they are ashes originating from the eruptive site itself as airborne pyroclastics – ash – that fell into the water and settled out. While some kinds of coarse ash can look exactly like this, the nearest known area of vents is 22 km away in East Haven, CT (94, 95), although there could have been vents closer a minimum of 7 km away. In definitive pyroclastics proximal to the Talcott eruptions, there are abundant accretionary lapilli – basically volcanic hailstones formed by the addition of moist ash around a central nucleus as it is in motion in air. Accretionary lapilli have not been found at this site.

We tend to favor the hyaloclastite hypothesis, but that it mostly occurred early in the extrusion of the Talcott, perhaps just as the flows were entering the water for the first time. However, the distinction between the two explanations is important because they speak to the explosiveness of the eruptions, and that is related to their effectiveness at transporting materials into the stratosphere where they could have global, as opposed to relatively local effects.

A meaningful sidelight is that the red beds with the graded beds are lacustrine, because it is water in which pillow lavas form. There is little to suggest that these sediments formed in a lake except a lack of evidences of exposure to air such as desiccation cracks or roots – but they did.

Beneath the graded beds of hyaloclastite or ash are red sandstones and siltstones lacking igneous debris. At some level below, there is the horizon of the ETE. This has yet to be specifically identified but present evidence suggest that it should be within 10s of meters below the layers exposed. Several prominent discoveries of reptile skeletal remains have been made in stratigraphic levels below the presumed position of the ETE in the Meriden area (Figure 22). These include the parareptile *Hypsognathus*, represented by a very handsome skull and partial skeleton, the afore-mentioned skull of the pseudosuchian *Erpetosuchus* (Figure 19), and a skull of the sphendontian *Colobops* (96-98). The former two forms are unknown outside strata of Late Triassic age, while the latter is represented by the still extant Tuatara of New Zealand. These finds indicate that the age of most of the New Haven Formation is in fact Late Triassic and pre-latest Rhaetian (the age of the ETE).



**Figure 21:** Graded beds of ?hyaloclastite in uppermost New Haven Formation from Stop 2. Yellowish clasts are altered basalt. (From 1).

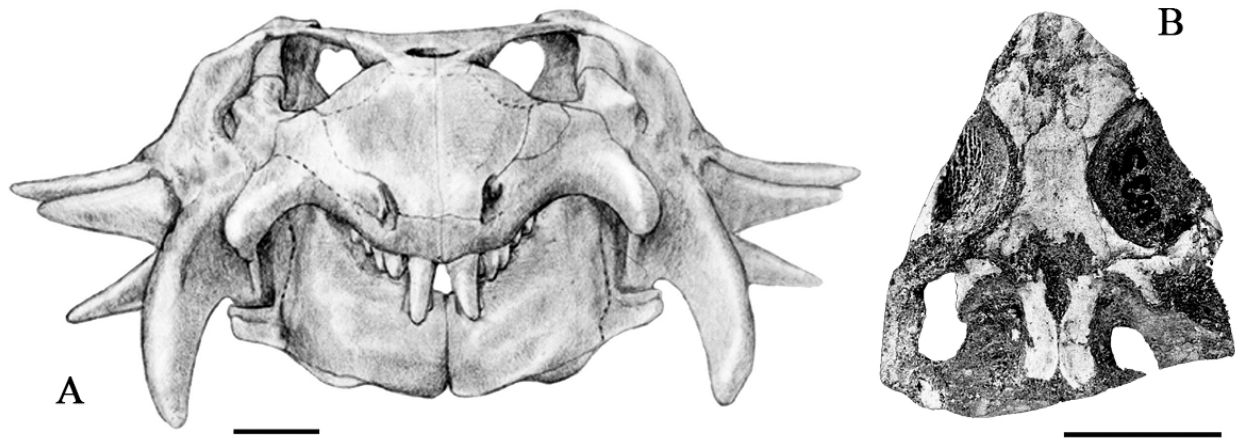


**Figure 22:** Triassic reptiles remains from the New Haven Formation of the Meriden area (scale bar is 1 cm): B, *Hypsognathus fenneri* from Meriden; C sphenodontian *Colobops* from Meriden [from refs. (1, 48, 92)].

**Advance of the lava flows.** Pillow basalts make up the most abundant kind of igneous rock on the Earth's surface because it forms at spreading ridges at mid-ocean plate boundaries, and comprises the upper part of 'Layer 2' of normal oceanic crust. Pillow basalts are also abundant around oceanic hot-spot volcanoes, such as those that formed the Hawaiian Islands. However, in both of these cases, the pillow basalts form very close to the vents sourcing the flows and fundamentally form flowing down-hill. Therefore, our understand may be not completely applicable to the CAMP flows into the rift basins, because they generally formed lava lakes in which the advancing flow can actually flow up-hill just like the waters' edge flows up the shoreline as a lake fills. This exposure presents a rare opportunity to examine features that help understand the dynamic behavior of this kind of pillowed flow.

The Talcott Formation comprises a complicated system of interbedded and intermixed flows, pillows complexes, breccias, and pyroclastics variably distributed in geography and vertically at any one site. The pillow complexes are present over most of the outcrop area. Pillows form by extrusion underwater from an aperture in the solidified crust of a much large flow lobe. The outside of a pillow chills very rapidly and then can itself rupture and extrude another pillow. Fundamentally, pillows form because the rapidity of cooling greatly limits their size, especially their diameter. Their along-flow length is also limited by the fast cooling, and hence it is impossible for pillows to extend far from a flow lobe. Therefore, there must have been streams of large lobes extending at least tens of kilometers, maybe hundreds, from the vents. Many lobes must have overrun earlier lobes and pillow complexes progressively from the vents outward and these may have been out of the water even as older lobes further out in the basin continued to exude pillows submerged. Insulation by burial by other parts of the flow complex may have allowed lobes to remain molten for protracted periods of time allowing them to extend for much greater distances than if they were surrounded by water.

Visible at these exposures are northeast tapering wedges comprising forests of pillowed basalt onlapping each other in the lower 10 m of the flow complex (Figure 20). These are easily traced by following red sandstone and siltstone beds that extend upward from the underlying New Haven Formation into the basalt. Locally pillows have foundered into the underlying sediment. Higher up in the Talcott Formation, amongst the wedges of basalt pillows, are larger bodies of massive

basalt without pillows some of which are over 6 m thick and scores of meters long. These are almost certainly examples of flow lobes that were the sources of the pillowed wedges. The direction of the local forests need not bear any specific relationship to the overall direction of progradation of the flow complex, because the forests could have come breaches on any side of the flow lobes.

Most of the uppermost Talcott here is highly vesicular, not pillowed and appears to have been deposited subaerially. With water displaced from this spot by underlying flows this may still be part of the same eruption as the underlying unit, despite being a separate cooling unit.

Assuming that the various pillow wedges and flow lobes represent one major eruptive event constrains the accumulation rate and water depth of the uppermost New Haven Formation. The couple or so meters of basalt-bearing sedimentary strata obviously took no more time to accumulate than the flow complex took to advance over the site, which was probably on the scale of days. The lake into which the lava poured had to be at least the depth of the high points of the individual wedges of pillowed basalt (i.e., 5 m or so), but probably not the depth of the entire Talcott Basalt because lava displaces water.

At a smaller scale, the typical geometries of basalt pillows are obvious here with concave upper surfaces and variously shaped bottom surface that conform to the underlying geometry. The glassy rinds of the pillows were altered by heated lake water and then deeper burial processes resulting clay formation and the release of materials reprecipitated as various mineral including zeolites that formed crystals in voids within the basalts complexes. These are much sought after by mineral collectors and their removal has resulted the big voids you see here and there along the face. The alteration of the glassy pillow rinds at this particular outcrop has been recently studied for insights into the study of volcanic rocks and lakes on Mars (99).

Looking closely at the rock face, you will see high angle cracks, irregular pockets, and flow-parallel contacts with red mudstone and basalt breccia fill, along with adjacent reddened basalt surfaces. Such red zones are often assumed to be fossil soils between flows, where they parallel flow contacts, injections from below, or violent mixtures of lava interacting with underlying sediment (pepparites) when they have other geometric relationships. If they were fossil soils they would indicate significant passage of time between flows, as is visible at the north end of the exposure. However, these red zones are actually infiltrated material coming down from above after the flows cooled. While none have yet been found here, these infiltrations often have reptile bones in them, because the open spaces they fill were good places for animals to live or get trapped in. PEO has found bones in such infilling in lava flows in Nova Scotia and New Jersey (100). It's a very important distinction because the more time there was between flows the more dilute the environmental impact was.

The simplest interpretation based on what is visible at this exposure is that the lava was prograding into a large, if not very deep, lake as a series of lava streams during one eruptive event. At the advancing front of these lava streams the cooling crust constantly ruptured, sending basalt pillows tumbling down in front and on their sides making cones and wedges of pillows. Eruption of these wedges shed hyaloclastite into the turbulent water into muds far in advance of the pillow wedges. After the lava flow system cooled, the voids were filled from above. Although the Talcott Formation is a relatively small flow system compared to the entire CAMP it was a part of the largest phase comprised of many eruptions spread over four major tectonic plates during an early phases of the igneous province that is the leading contender to have caused the ETE.



**Figure 23:** Characteristic prismatic fracture of the lower part of flow 2 of the Holyoke Basalt. Location is 42.007423°, -72.727982° in West Suffield, CT. The pattern is typical of the second flow almost everywhere, including the Meriden area. The origin of this fracture pattern is not understood but is clearly distinct from cooling fractures. From (1).

**Lavas of the Holyoke Basalt:** The Talcott Basalt Formation is overlain by the lacustrine Shuttle Meadow Formation. That unit is well known for very well-preserved fossil fish found in carbonate-rich deep-water lake sediments. That formation is not exposed here, however, buried by talus and soil. It underlies the shelf in the landscape as you look up and west toward the hill. In that direction you can see cliffs of Holyoke Basalt, the thickest lava flow formation in the Connecticut Valley Rift Basin. The lower part of the second flow of the Holyoke visible here, has a very interesting and distinctive splintery fracture (Figure 23) that along with several other unique features makes it possible to recognize this one flow from northern Massachusetts to central Virginia, a linear distance of over 700 km. Assuming just what is preserved, plus the intervening areas that have now eroded, yields a volume of over 2400 km<sup>3</sup> as a minimum estimate of this one eruptive event that probably lasted less than 100 years. For comparison, the Laki eruption in Iceland of 1783 and 1784, which by some estimates killed indirectly by global dimming and consequent crop failures, famine, disease and war (including the French Revolution) more than 5 million people (101), was only 15 km<sup>3</sup> in total (102). Yet, the Holyoke Basalt, although well constrained is only a small part of the CAMP.

### **Stop 3: The Inverted Pyramid – Dinosaur State Park (Lunch)**

Location: 41.651887, -72.656877 (Display Building of Dinosaur State Park, Rockyr Hill, CT)

Unit: East Berlin Formation

Time: ~200.99 Ma – Early Jurassic (Early Hettangian)

Environments: Shallow lake over deep lake

Highlights: Hundreds of dinosaur footprints, few herbivores

Leave the vehicle and proceed to the Dinosaur State Park (DSP) Exhibit Center (EC).

The spectacular trackways at DSP were uncovered in 1966 during the excavations for a state building (Figure 24). Sidney S. Quarrier of the Connecticut Geological Survey, Joe Webb Peoples from Wesleyan, and John H. Ostrom of Yale, among others, recognized the importance of the finds



**Figure 24:** Original excavation of *Eubrontes giganteus* trackways at DSP in 1966. From (1).

and quickly acted to protect the site and worked to have the site preserved as an in situ display in a state park (103). Subsequently, a large track-bearing surface was preserved beneath the DSP EC where they are visible today, while the larger original discovery surface was reburied for possible future exhibit. DSP is today one of the most popular parks in Connecticut attracting some 50,000 visitors a year, and *Eubrontes giganteus*, by far the most abundant track at the site, is now the Connecticut state fossil (Figure 25).



**Figure 25:** Natural Cast in sandstone of a typical *Eubrontes giganteus* from Dinosaur State Park. Quarter is 24.3 mm in diameter. From (1).

Since its discovery, the largely gray strata comprising the footprint-bearing interval in DSP has been recognized as being located in the upper East Berlin Formation as is clear from physical proximity of the overlying Hampden Basalt. Short rock cores (104, 105) taken at the site early in its history show that the footprint layers lie closely above a well-developed black shale, indicating that the tracks occur in the over-all regressive phase of the orbitally-paced lake laminated mudstone. Based on the recent quadrangle mapping in this area (106), given a dip of  $11^\circ$  and a map distance of 220 m from the track bed to the mapped base of the Hampden Basalt, the track sequence may lie about 42 m below the basalt which shows that the track bed in is third black-shale-bearing cycle below the basalt (Figure 16, **Stop 4**), although this is far from certain and needed to be verified by coring.

What appears to be the same black mudstone underlying the track beds at the park was encountered in an excavation along West Street just west



**Figure 26:** Largely dephosphatized *Semionotus* from the laminated mudstone below the track beds at DSP found at excavation along West Street. Scale is 1 cm. N.G. McDonald collection. From (1).

of the service entrance for the park. N.G. McDonald found several mostly dephosphatized *Semionotus* (Figure 26) and many clam shrimp in the rubble heaps with preservational modes similar to those in the Westfield Fish Bed (**Stop 4**). These make a nice addition to the park's fossil assemblages.

**Inverted ecological pyramid:** As seen at the DSP post-ETE track assemblages are overwhelmingly dominated by the tracks of carnivores. The DSP track level is at about 201.0 Ma in the Early Hettangian of the Early Jurassic, only half a million years after the end-Triassic-extinction. As noted in the introduction, this reflects a post-mass extinction tetrapod community that was water-based with

the theropods subsisting largely on fish and other carnivores.

*Eubrontes* was made by a theropod dinosaur. Reconstruction of the osteology of the foot using the “arthral” method, in which pads are assumed to underlay the joints, results in a skeleton that is very similar to the Early Jurassic theropod *Dilophosaurus* from the Kayenta Formation of Arizona (Figure 27) (8). A full size model of this dinosaur is on display at DSP in a diorama next to the tracks. This model was made before it was known that non-avian dinosaurs were feathered. A more recent model (Figure 28) (107) shows *Dilophosaurus* covered with “protofeathers” consistent with the phylogenetic bracket analysis looking very similar to the Early Cretaceous tyrannosaur *Yutyrannus* preserved with protofeathers (38). (8)

The vast majority of tracks found in the post-ETE latest Triassic and Early Jurassic strata in Eastern North America were made by theropods, the tracks of which are collectively called brontozoids. Some herbivore tracks are present such as *Anomoepus* and *Otozoum*, but they are rare. In contrast middle and Late Jurassic and Cretaceous track assemblages are often comprised of track assemblages in which herbivorous dinosaur tracks are more abundant than carnivorous forms (108). Inasmuch as the assemblages at our field stops post-date one of the largest mass-extinctions of all time, the end-Triassic extinction, the terrestrial ecosystems were anything but normal. A strong case has been made that Early Jurassic brontozoid tracks from the Moenave Formation, Utah

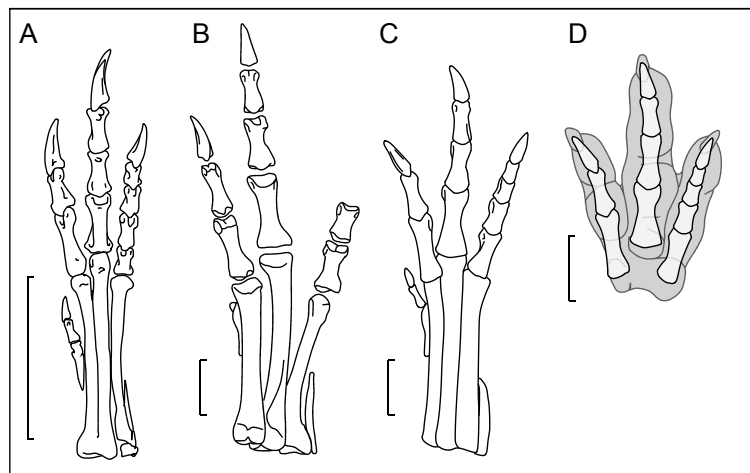


**Figure 27:** Osteological reconstruction and comparisons with osteological taxa of the holotype of *Eubrontes giganteus* at the Beneski Museum AC 15/3: A, right pes of *Megapnosaurus* (*Syn-tarsus*) *rhodesiensis* ; B, *Dilophosaurus wetherelli*, right pes; C, *Dilophosaurus wetherelli*, reconstructed right pes; D, arthral model reconstruction of the holotype *Eubrontes giganteus*, AC 15/3; Scale is 10 cm. From (1, 45).

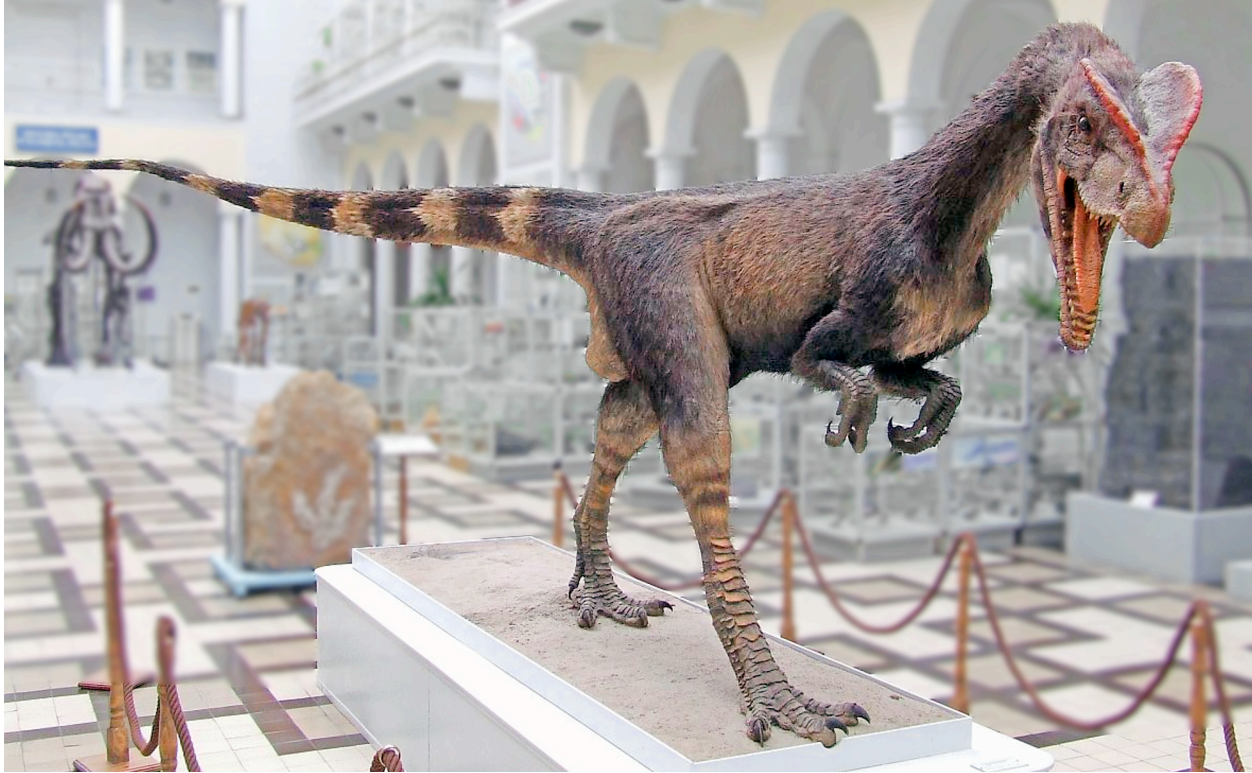


**Figure 28:** *Dilophosaurus* as reconstructed in the Geological Museum of the Polish Geological Institute, Warsaw. From (1).

(an assemblage that looks remarkably like that from the Connecticut Valley) were made by theropod dinosaurs that subsisted largely on fishes (48, 109), as do many extant dinosaurs (birds). This is supported by the presence of the teeth of *Dilophosaurus* and isolated teeth found with the Moenave tracks that are similar to those of known theropod piscivores such as the spinosaurids, with which they also share snout adaptations with. Similar, though smaller, teeth have been found in lacustrine strata in the Connecticut Valley Rift Basin (109) (Figure 29). With a water-based economy, theropods could be proportionally much more abundant than if they subsisted on herbivorous dinosaurs alone. Additionally, the end-Triassic extinction wiped out all the tropical semiaquatic carnivores, such as phytosaurs and large labyrinthodont amphibians, so theropods had few or no competitors at the waters edge. The crocodylomorphs were comparatively small (~1 m) and were more likely prey than competition. Thus, the “Eltonian” or ecological pyramid (109-112) of the Early Jurassic terrestrial realm had its base in the water and that is why it appears to be upside down. Similar water-based terrestrial communities must have existed when tetrapods first moved onto land. It would not be until the late Early Jurassic and Middle Jurassic that herbivores became more common than carnivores, and the typical terrestrial trophic pyramid was re-established.

Recent work at DSP has concentrated at digitally rendering the trackways in 3 dimensions so that they can be quantitatively analysed in more objective manner using morphometric methodologies (8). This includes



**Figure 29:** Theropod dinosaur tooth from the Shuttle Meadow Formation. N.G McDonald collection. From (1).

digitally remapping the exposed track bed as well as the ability to 3d print specimens at any size.

Note that the DSP EC has many other kinds of tracks from other localities (such as *Otozoum*), as well as well fish and plants on display that should be examined. One of these is a recently discovered trackway of the mammal-like ichnotaxon *Ameghinichnus* (Figure 30), also known from the Newark Basin (6, 113). Close mammal relatives and early mammals have very conservative foot structure and there are a number of Early Jurassic forms that could have made these tracks. Actual known mammaliforms from the Early Jurassic are too small to have made these footprints, but tritlodonts and tritylodonts were the right size and are known from skeletal remains from the Fundy Rift Basin (112, 114).



**Figure 30:** *Ameghinichnus* from the middle Shuttle Meadow formation of Berlin, CT. From (1).

#### **Stop 4: Time Keeper of the Solar System and Pacemaker of Life**

Location: 41.622162, -72.740125 (service lane on right side of entrance ramp for CT-9 south from CT-15, East Berlin Formation)

Units: East Berlin Formation and Hamden Basalt

Time: ~201.0 Ma – Early Jurassic (Early Hettangian)

Environments: Fluvial and shallow to deep lacustrine and flood basalt

Highlights: Milankovitch and lacustrine cycles, giant lakes, fossil fish and species flocks, fish taphonomy and sediment deformation, comparison to Mediterranean sapropel sequences.

After parking, we will walk east on the south side of the road going up section (east) along the outcrop until we reach the Hampden Basalt, taking care not to stray onto pavement. Once there we will look at the basalt and then walk down through the sedimentary section focusing on the highlights. Once again, a permit from CT DOT is needed for a visit to this stop.

The highway cut at East Berlin at the intersection of US-15 and CT-9 and a similar cut at the intersection with I-91 reveal fault-repeated sections of the upper 2/3 of the East Berlin Formation. The lacustrine sedimentary cyclicity of this section was first recognized in the 1950s (115, 116) and commented on by many subsequent workers. Olsen hypothesized that the East Berlin cyclicity was paced by Milankovitch cycles in 1986 (117), and that has been highly corroborated by U-Pb radiometric dates in 2013 (61)). In fact, this section is nearly a cartoon of Milankovitch cycles, albeit on a huge scale (Figure 16), and its obviousness, itself calls for an explanation.

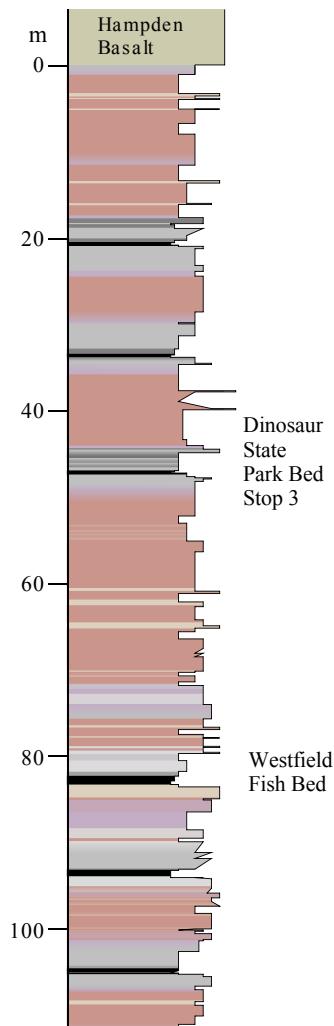


**Figure 31:** Upper East Berlin Formation and Hampden Basalt at Stop 4. From (1).

About 117 m of sedimentary section is exposed on the south side of the cut (Figure 31). The most obvious cycles have a well-developed dark gray to black laminated deepest water interval exemplified by the cycle bearing the Westfield Fish Bed (Figure 32). Similar meter-scale lithological cycles were described by Van Houten in the 1960s in the Triassic age Lockatong Formation of the Newark Rift Basin (NY, NJ, PA) and interpreted as lake level cycles paced by the precession cycle, and this was at a time that the Milankovitch theory of the Ice Ages was thought by many to be “disproven”. PEO named this type of transgressive-regressive cycles after Van Houten in 1986 (117). To facilitate description and discussion, Olsen (117) described Van Houten Cycles as comprised of three divisions defined relative to each other: Division 1, lake transgression; Division 2, lake high stand; and Division 3, lake regression and low stand. Each division is recognized by suites of sedimentary features indicative of the relative sense of water depth change, such as an upward decrease and disappearance of desiccation cracks in a Division 1; followed by finely laminated mudstone of Division 2. Division 3 will show the opposite sense of change with the reappearance of signs of shallow water such as desiccation cracks and roots. In the case of the cycle bearing the Westfield Fish Bed, these transitions and divisions are easy to recognize and they are accompanied by very obvious color changes. But in some other cycles the changes are more subtle and sometime with no color changes. It is important to realize that these cycles are defined by the *relative* sense of change not absolute kinds of sedimentary rock.

**Hampden Basalt:** We begin our traverse at the Hampden Basalt, which is representative of the youngest known CAMP flows known in eastern North America and Morocco, although there are hints of a younger eruption based on a fourth CO<sub>2</sub> pulse in the Portland Formation (3). The basalt is typically massive but is vesicular at its base.

Tilted pipe-stem vesicles are common at the lower contact and seem to indicate a northeasterly flow direction (118). A known feeder for the Hampden basalt is the Black Rock diabase dike of Massachusetts. The visible thermal effects of the flows are minimal, restricted to the upper meter of the East Berlin. The Hampden Basalt is the thinnest of the extrusives in the Hartford basin, reaching a maximum thickness of 30 m, but interestingly is seemingly associated with one of the largest magnitude CO<sub>2</sub> pulses (Figure 7). It is also one of the most widespread flows known in the CAMP, extending from the Connecticut Valley Rift to the Newark Rift and possibly to Morocco where it is known as the “recurrent basalt formation”, although that remains to be tested. The age of the Hampden Basalt is  $200.916 \pm 0.064$  based on correlation to U-Pb - dated intrusions (61).

**Cyclicality and Comparison to the Present:** Perhaps the most remarkable aspect of this outcrop is the very obvious cyclicality tied to Milankovitch climate change. Pacing of climate celestial mechanical variations was first clearly demonstrated in the Quaternary and amazingly we can make

a close comparison between this sequence and the Quaternary (Figure 16). In particular, the pattern of Mediterranean sapropels as seen in cores and outcrops is very close to that seen here, despite the fact the Mediterranean is a sea and marine, these strata are continental, and the mechanism is very different. Sapropels are organic-rich muds or mudstones generally interpreted as being deposited below anoxic water. The hydrodynamic and climatic origin of these sapropels in the Mediterranean is debated, but there is agreement that their proximal cause is chemical and density stratification of water column that is close in time to intervals of maximum insolation in overall times of highest precessional variability, that is, times of high orbital eccentricity. Recent modelling suggests that the stratification was generated by a reduction in the supply of oxygenated bottom water, however, the precise mechanisms appear involve a complex interplay between regional and large-scale climatic patterns, such as warming, sea-level rise, insolation-driven enhanced African run-off, and ocean-biogeochemical mechanisms, such as enhanced late glacial nutrient content and major shifts in the pelagic ecosystem structure. Despite this apparent complexity, the sapropel pattern is remarkably simple and looks very much like this section. This is true in terms of the general pattern, but also in the strong and unexpected obliquity power (Figure 17). The conceptual model for the East Berlin or of the Eastern North American lacustrine cycles is exactly anti-phased at the precessional scale compared to the sapropels, but in-phase at the eccentricity scale in terms of insolation, with deeper lake occurring during times of maximum insolation.

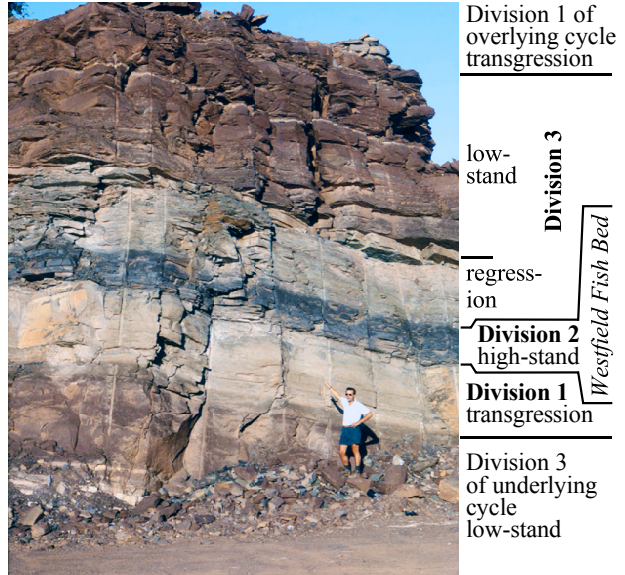


**Figure 32:** Cycle with the Westfield Fish Bed and Pompton Ashes with Peter LeTourneau for scale in 1985. From (1).

**First 100 kyr Before the Hamden Basalt and the Dinosaur State Park Bed:** As we walk west and down-section, you will see red strata below the basalt and then there is an interval of no exposure. Looking across the highway, you can see there is an equivalent gap there as well. This gap is a glacially scoured valley that has followed the uppermost of the black shale-bearing cycles in the East Berlin. We know this because the upper 50 m of the formation is more completely exposed at the interchange for I-91 about 3.8 km east and that section has been used to fill in the gap (63). The next cycle down also has a black shale, as does the one below that. The latter, the third black-shale-bearing cycle from the top, may be the unit that is exposed at Dinosaur State Park (*Stop 3*) (Figure 31), the main footprint layer that is the gray regressive part of Division 3 of this cycle. Together these three cycles along with the redbeds underlying the basalt comprises a most of a ~100 kyr short eccentricity cycle, with the last 20 kyr or so of that larger cycle being in the basal Portland Formation overlying the Hampden Basalt.

**Low Variability in a Short Eccentricity Cycle:** Walking further to the west and down-section, we encounter a long section of red beds. There is a thin-bedded red interval with some interbedded tan sandstone beds at about at about 62 m in Figure 18. This is a very weakly developed division

2 deposited during a time of low precessional-scale variability corresponding to low eccentricity in a ~100 kyr cycle. At roughly 75 m in Figure 31, there is a purplish siltstone and sandstone, much more visible on the north side of the entrance ramp, that represents a slightly better developed Division 2 of a cycle, still with n the interval of low eccentricity.

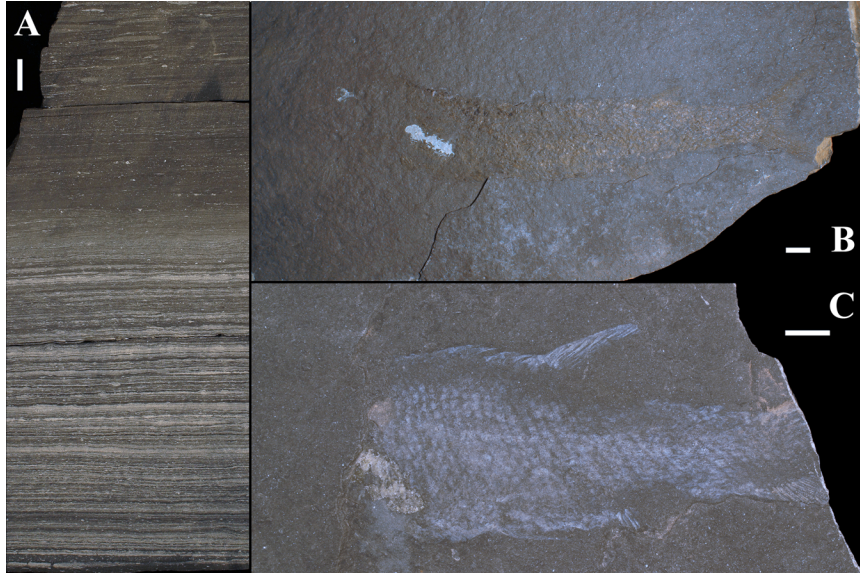


**Figure 33:** Westfield Fish Bed and dephosphatized fish. A, Micro-laminated mudstone passing upward into sedimentary melange. B, Complete *Redfieldius* represented only by an organic film head is not visible. C, Complete *Semionotus* revealed by calcite film. In both AB and C head is not visible because of extreme dephosphatization. Scale is 1 cm. From (1).

forms), *Diplurus* cf. *longicaudatus* (a coelacanth), and *Ptycholepis* (another paleonisciform, that has been found at another site) (Figure 34). The Westfield Fish Bed produced the one of the very first recorded discoveries of articulated fossil fish in North America, a *Redfieldius* from Westfield, CT, mentioned by Silliman in 1816 (119). The *Semionotus* species from this bed have a very wide range of body forms and scale shapes and comprised species flocks, similar to the cichlid fishes of the East African great lakes (120).

The fish here, as at most localities of the Westfield Fish Bed, are to varying degrees “dephosphatized” (Figure 33); that is, the phosphate mineral matter of the bone has been mostly or completely dissolved early in diagenesis by microbially mediated post-burial processes (121-123). This can lead to complete disappearance of the fish or just the faintest of “ghost fish” may remain. That this is not due to acidity is shown by the fact that calcitic fossils (such as charophytes) are well preserved and carbonates are more soluble than phosphates under acidic conditions alone. This dephosphatization is almost certainly a very much more wide spread phenomena than realized (124) and in fact may be the norm rather than the exception.

**Westfield Fish Bed:** At roughly 82 m below the Hampden Basalt is Division 2 of the cycle depicted in Figure 31. This Division 2 is the Westfield Fish Bed, This bed has a calcareous, organic-rich, microlaminated interval that has abundant, if oddly preserved, fish (Figure 33 and Figure 34) bivalve crustaceans and also contains the Pompton Ashes (Figure 9 and 35).

In order of abundance, the Westfield Fish Bed has produced *Semionotus* spp. (holostean gar relatives), (holostean gar relatives), *Redfieldius* spp. (paleonisciforms),

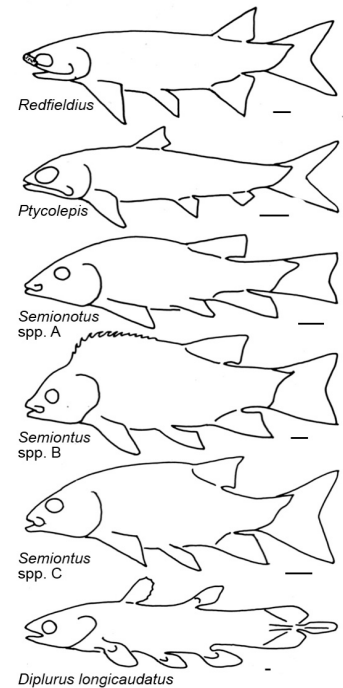


**Figure 34:** Fish taxa from the Westfield Fish Bed. From (1).

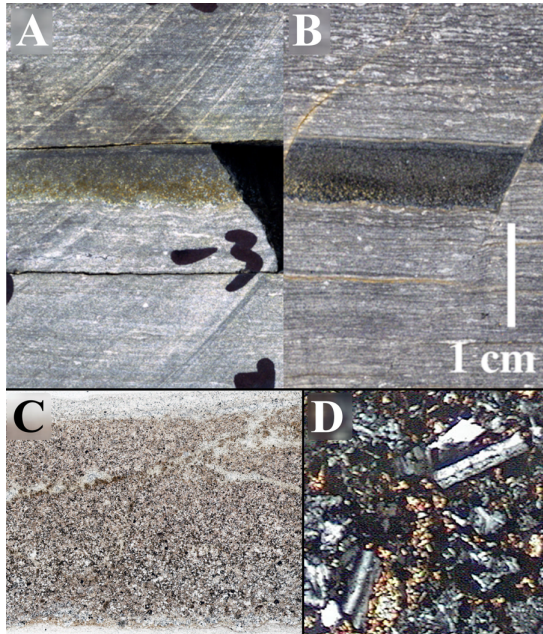


**Figure 35:** Lower Pompton Ash: A, Army Corps of Engineers C-128 Core in the Towaco Formation, with the Pompton Tuff being the ~0.5 cm dark graded layer; B, East Berlin Fm. at Parmelee Brook about 130 km away in the Connecticut Valley Rift Basin; C, Thin section of the Pompton, Tuff at Stop 4, with thickness of layer at 6.8 mm and largest particles at base of layer are 0.15 mm; D, thin section with euhedral plagioclase laths 0.1 mm long with a high aspect ratio, showing no signs of rounding. Originally they were enclosed in glass that is now converted to a clay or chalcedony. From (1).

Also present in the Westfield Fish Bed are *Bulblimnadia* sp. clam shrimp (spinocaudatan bivalved crustaceans), carbonate parts of charophyte green algae, and land plant fragments of various sizes.

**Giant Chemically Stratified Lakes:** The Westfield Fish Bed is representative of a specific facies that normally preserves whole fish and sometimes terrestrial vertebrates and insects. The microlaminated strata of this bed are comprised of carbonate rich and carbonate poor laminae forming couplets most simply interpreted as annual in origin – that is they are lacustrine varves. Today these kinds of sediments form in bodies of water that perennially have no oxygen at depth because the area of the water body is small compared to its depth and therefore the work of the wind does not mix the lake (125). Individual couplets and patterns of couplets are traceable over extent of the Westfield Fish Bed. This indicates that wave base never intersected the bottom during deposition of the bed, which is consistent with the lake being perennial stratified. Given the minimum length of the strata not exposed to wave base (~ >100 km) and a range of reasonable wind speeds, the Westfield Fish Bed was deposited in lake a minimum of about 50 m (125) with an anoxic hypolimnion. There is some evidence that the lake in which the Westfield Fish Bed was deposited extended into the Newark Basin. Similar strata are present in the Culpeper Rift Basin of Virginia as well. If the lake extended that far, it would be in excess of 700 km long, making it larger than any present lake, save the Caspian and Black Seas.

**The Pompton Ashes and CAMP Mega-eruption:** The lower 10 cm of the Westfield Fish Bed has a thin, graded basaltic crystal tuff and an overlying similar but thinner ash collectively called the Pompton Ashes (18), named for an outcrop in Pompton, NJ in the correlative Towaco Formation (Figure 9). The graded, apparently basaltic to andesitic ash consists of euhedral, non-rounded, plagioclase laths in clay or chalcedony matrix that was originally glass, fine-grained feathery feldspars, carbonate, and distinct sub-mm spherule-like volcanic grains at the base. Pyrite is abundant and can comprise more than 20% of the bed by weight (20). Consequently, the ash weathers to an expanded bright orange jarositic mush. The pyrite is most simply explained as having formed in the pore space of the ash after deposition, rather than part of the ash itself. At this outcrop, the surface of the ash is often orange, but if you break off a piece the inside is dark gray.

Thus far, the Pompton ash has been found at 10 localities, 7 (2 cores and 5 outcrops) in the Hartford Subbasin of the Connecticut Valley Rift Basin and 3 (2 cores and 1 outcrop) in the Newark Rift Basin, spread out over a distance of about 200 km (Figure 9). Several aspects of this ash

are surprising. First, its thickness does not change over its 10 known sites and 200+ km extent, implying it is either the product of a huge, distant eruption, or a smaller eruption closer and positioned just-so. Second, the upper ash is a <1 mm lamina a few cm higher that also does not change thickness. Third, while validating that ~30-year-old lake cycle correlations between basins are shown correct by the presence of these ashes, it is astounding that these ashes are enclosed by congruent patterns of microlaminae over the same distances. This implies either that the Newark and Hartford basins could have been connected in a single giant rift lake, as suggested above, or that seasonal to centennial climatic variations overrode all other sources of sediment variability, or both. It is noteworthy that no such correlation has been described for separate extant lakes. Fourth, as has been seen in some basaltic ashes, the lower Pompton Ash has a modest Ir anomaly, suggesting similar ashes might be the source of more cryptic Ir anomalies in other Triassic-Jurassic strata. Finally, fifth, not only can we evidently correlate strata among various Triassic-Jurassic basins at the 20 kyr cycle level, for some intervals we can confidently also correlate at the seasonal scale. We know the year, even the season of the eruptions.

As discussed above (Figure 12),  $\delta^{34}\text{S}$  in pyrite in the laminate around the Pompton Ashes exhibit pronounced negative values (20) providing evidence that they fertilized the lake with volcanic sulfate. This sulfate, while still in the upper atmosphere, would have caused a volcanic winter via enhanced albedo — one for each of the ashes.

The Pompton Ash is likely part of the CAMP as it is andesitic to basaltic in composition. It does not change thickness over a distance of 200 km suggesting that it is a distal product of a giant Yellowstone-scale mega eruption very far away, like south Florida a possible center of the CAMP plume. Despite the suggestion that this ash is the result of a mega-eruption it was but a puny part of the CAMP, one of the largest eruptive complexes on Earth.

**Melange:** Overlying the micro-laminated part Westfield Fish Bed is an odd unit consisting a *mélange* of small (usually <20 cm) quadrangular to rounded or folded clasts with truncated oblique-to-bedding laminae floating in a poorly-bedded matrix (Figure 36). In 1989 (63), PEO half-jokingly termed the clasts “dead horses” (derived from “horse” for a fault-bounded sliver of rock and its flattened or prone position), hoping in vain to provoke interest. When noted at all, “dead horse” *mélanges* have been interpreted as depositional units such as turbidites, rip-up clasts indicating subaerial exposure, slumps, or seismites, but PEO argues that they are “early” shear and dewatering-related units that did not have a free surface at the time of deformation

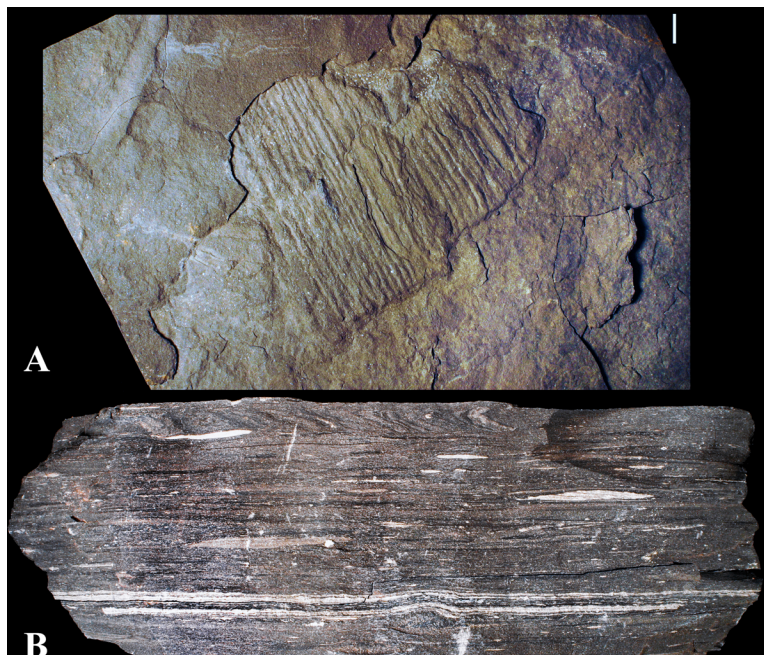


**Figure 36:** Early post-depositional bedding-plane-parallel mélanges created by shear and liquefaction: A, plan view; B, cross-section. From (1).

(126). These are actually very common; in lacustrine sequences of the Triassic-Jurassic of the eastern US, nearly every sedimentary cycle with a dark gray to black mudstone has such a layer, amounting to hundreds of beds, including all of the black shales at this site. Similar beds are abundant in the Eocene Green River Formation [e.g., (127)] and are found in many other organic-rich, laminated mudstone sequences, although they are invariably interpreted as depositional units.

Assuming these mélanges are depositional leads to very serious mistakes in environmental interpretation. Moreover, because they formed post-depositionally, between pre-existing beds, and their formation was controlled by a combination of specific rheology at unknown depths and pressures (with or without specific triggers) each bed cannot be treated as resulting from a specific event, and a stratigraphy of sequential beds cannot be interpreted as a history of events.

It is a serious mistake to interpret every layer one sees as a historical event – sometimes the main feature of a sedimentary unit are post-depositional and the appearances are a result of their rheology under stress not their sedimentology.

***The rest of the section:*** Continue walking to the west and examine two more Van Houten cycles, each with a black shale-bearing division 2. The middle cycle has a bedding plane fault that has chewed up most of the laminated portion of Division 2. The lowest cycle has a division 2 with numerous crystals of magnesite (magnesium carbonate) (128). The significance of these crystals is not clear and it is possible that they represent a relatively local diagenetic effect. Most of the division 2 does not appear to be well laminated, however the base is and those laminae are traceable at least 5 km to the southeast.

## **Acknowledgements**

Our thanks to Nick McDonald and Peter LeTourneau who generously shared their knowledge and materials. Thanks to the land owners and agencies who allow us to visit the field stops, especially Dinosaur State Park (Michael Ross), the Connecticut Department of Transportation, and the Meriden Target store. Much of this field guide is derived from a field trip guidebook for a trip sponsored by the Keck Foundation and hosted by Wesleyan University (1) for which PEO is grateful. We also thank IODP for making this fieldtrip possible as well as the participants for making the trip intellectually stimulating. Sean Kinney, Clara Change and Bennett Slibeck, are thanked for their help during the fieldtrip and discussions that substantially influenced and improved the guidebook. This is a contribution to Project 4 of CycloAstro funded by the Heising-Simons Foundation (award no. 2021-2801).

## References

1. P. E. Olsen, *Origins of Dinosaur Dominance in the Connecticut Valley Rift Basin*, A Field Trip Sponsored by the Keck Foundation & Hosted by Wesleyan University, Keck Geological Consortium (Wesleyan University, Middletown, CT, 2017).
2. M. F. Schaller, J. D. Wright, D. V. Kent, A 30 Myr record of Late Triassic atmospheric  $p\text{CO}_2$  variation reflects a fundamental control of the carbon cycle by changes in continental weathering. *Geological Society of America, Bulletin* **127**, 661-671 (2015).
3. M. F. Schaller, J. D. Wright, D. V. Kent, P. E. Olsen, Rapid emplacement of the Central Atlantic Magmatic Province as a net sink for  $\text{CO}_2$ . *Earth and Planetary Science Letters* **323**, 27-39 (2012).
4. M. F. Schaller, J. D. Wright, D. V. Kent, Atmospheric  $p\text{CO}_2$  perturbations associated with the Central Atlantic magmatic province. *Science* **331**, 1404-1409 (2011).
5. J. C. McElwain, D. J. Beerling, F. I. Woodward, Fossil plants and global warming at the Triassic-Jurassic boundary. *Science* **285**, 1386-1390 (1999).
6. P. E. Olsen *et al.*, Arctic ice and the ecological rise of the dinosaurs. *Science Advances* **8**, eabo6342 (2022).
7. M. Pole *et al.*, The rise and demise of *Podozamites* in east Asia—An extinct conifer life style. *Palaeogeography, Palaeoclimatology, Palaeoecology* **464**, 97-109 (2016).
8. P. R. Getty *et al.*, Exploring a real Jurassic Park from the dawn of the Age of Dinosaurs in the Connecticut Valley. *Geological Society of Connecticut, Guidebook* **9**, 1-82 (2017).
9. S. Kinney *et al.*, Onset of long-lived silicic and alkaline magmatism in eastern North America preceded Central Atlantic Magmatic Province emplacement. *Geology* **in press** (2022).
10. S. Kinney *et al.*, Development of High-resolution Paleoclimate Dataset from Whole Rock Geochemistry of Two Continuously Cored Mesozoic Continental Sequences. *AGU Fall Meeting 2022 Abstract Submitted* (2022).
11. S. T. Kinney *et al.*, The White Mountain Magma Series (New Hampshire, USA): A CAMP-related episode of silicic and alkaline magmatism? *for Geology submitted* (2021).
12. M. Lustrino *et al.*, Origin of Triassic magmatism of the Southern Alps (Italy): Constraints from geochemistry and Sr-Nd-Pb isotopic ratios. *Gondwana Research* **75**, 218-238 (2019).
13. M. J. Benton, Diversification and extinction in the history of life. *Science* **268**, 52-58 (1995).
14. A. Berger, M. F. Loutre, "Precession, eccentricity, obliquity, insolation and paleoclimates" in Long-Term Climatic Variations, J. C. Duplessy, M.-T. Spyridakis, Eds. (Springer, Berlin, Heidelberg, 1994), vol. 122, pp. 107-151.
15. M. F. Schaller, M. K. Fung, J. D. Wright, M. E. Katz, D. V. Kent, Impact ejecta at the Paleocene-Eocene boundary. *Science* **354**, 225–229 (2016).
16. J. H. Whiteside *et al.*, Extreme ecosystem instability suppressed tropical dinosaur dominance for 30 million years. *Proceedings of the National Academy of Sciences* **112**, 7909-7913 (2015).
17. P. E. Olsen *et al.*, CAMP ashes and the ETE. *Goldschmidt 2017 Abstracts*, <https://goldschmidt.info/2017/abstracts/abstractView?id=2017006082> (2017).
18. P. E. Olsen *et al.*, Wild and wonderful implications of the 5 mm Pompton Ash of the Hartford and Newark basins (Early Jurassic, Eastern North America). *Geological Society of America Abstracts with Programs* **48**, doi: 10.1130/abs/2016NE-272509 (2016).
19. M. Et-Touhami *et al.*, Tectonic, astrochronostratigraphic, and biostratigraphic implications of the paleomagnetic polarity reversal stratigraphy of the Late Triassic Bigoudine Formation (Argana Basin, Morocco). *AGU, 2016 Fall Meeting Abstracts*, GP43B-1251 (2016).
20. E. E. Stüeken *et al.*, Effects of pH on redox proxies in a Jurassic rift lake: Implications for interpreting environmental records in deep time. *Geochimica et Cosmochimica Acta* **252**, 240-267 (2019).
21. P. Olsen *et al.*, Two CAMP Explosive Eruptions. *Goldschmidt Abstracts* **2019**, 2511: <https://goldschmidtabstracts.info/abstracts/abstractView?id=2019005267> (2019).
22. C. S. Lane, C. M. Martin-Jones, T. C. Johnson, A cryptotephra record from the Lake Victoria sediment core record of Holocene palaeoenvironmental change. *The Holocene* **28**, 1909-1917 (2018).

23. M. C. McCanta, R. G. Hatfield, B. J. Thomson, S. J. Hook, E. Fisher, Identifying cryptotephra units using correlated rapid, nondestructive methods: VSWIR spectroscopy, X - ray fluorescence, and magnetic susceptibility. *Geochemistry, Geophysics, Geosystems* **16**, 4029–4056 (2015).
24. T. Matsu'ura, T. Ueno, A. Furusawa, Characterization and correlation of cryptotephra using major-element analyses of melt inclusions preserved in quartz in last interglacial marine sediments, southeastern Shikoku, Japan. *Quaternary international* **246**, 48-56 (2011).
25. C. T. Griffin *et al.*, Africa's oldest dinosaurs reveal early suppression of dinosaur distribution. *Nature*, 1-7 (2022).
26. D. V. Kent, L. B. Clemmensen, Northward dispersal of dinosaurs from Gondwana to Greenland at the mid-Norian (215–212 Ma, Late Triassic) dip in atmospheric *p*CO<sub>2</sub>. *Proceedings of the National Academy of Sciences* **118**, e2020778118 (2021).
27. T. H. Huxley, On the animals which are most nearly intermediate between birds and reptiles. *Annals and Magazine of Natural History* **2**, 66-75 (1868).
28. R. T. Bakker, P. M. Galton, Dinosaur monophyly and a new class of vertebrates. *Nature* **248**, 168–172 (1974).
29. G. S. Paul, *Predatory Dinosaurs of the World: A Complete Illustrated Guide* (Simon & Schuster, New York, 1988), pp. 464.
30. A. Feduccia, *Romancing the Birds and Dinosaurs: Forays in Postmodern Paleontology* (BrownWalker Press, Irvine and Boca Raton, 2020), pp. 408.
31. A. G. Sharov, Novyiye lyetayushchiye reptili iz mezozoya Kazakhstana i Kirgystana [New flying reptiles from the Mesozoic of Kazakhstan and Kirgystan] *Trudy paleontologicheskii institut, Moskva (Proceedings of the Paleontological Institute, Moscow)* **130**, 104–113 (1971).
32. K. R. Jäger, H. Tischlinger, G. Oleschinski, P. M. Sander, Goldfuß was right: Soft part preservation in the Late Jurassic pterosaur *Scaphognathus crassirostris* revealed by reflectance transformation imaging (RTI) and UV light and the auspicious beginnings of paleo-art. *Palaeontologia Electronica* **21**, 1-20 (2018).
33. G. A. Goldfuss, Beiträge zur kenntnis verschiedener reptilien der vorwelt. *Nova Acta Physico-Medica Academiae Caesareae Leopoldino-Carolinae Naturae Curiosorum* **15**, 61-128 (1831).
34. Z. Yang, Jiang, B., McNamara, M.E., Kearns, S.L., Pittman, M., Kaye, T.G., Orr, P.J., Xu, X. and Benton, M.J., , Pterosaur integumentary structures with complex feather-like branching. *Nature ecology & evolution* **3**, 24-30 (2019).
35. A. Cincotta *et al.*, Pterosaur melanosomes support signalling functions for early feathers. *Nature* 10.1038/s41586-022-04622-3 (2022).
36. F. V. Paladino, M. P. O'Connor, J. R. Spotila, Metabolism of leatherback turtles, gigantothermy, and thermoregulation of dinosaurs. *Nature* **344**, 858–860 (1990).
37. M. J. Benton, Z. Zhonghe, P. J. Orr, Z. Fucheng, S. L. Kearns, The remarkable fossils from the Early Cretaceous Jehol Biota of China and how they have changed our knowledge of Mesozoic life: Presidential Address, delivered 2nd May 2008. *Proceedings of the Geologists' Association* **119**, 209-228 (2008).
38. X. Xu *et al.*, A gigantic feathered dinosaur from the Lower Cretaceous of China. *Nature* **484**, 92-95 (2012).
39. X.-T. Zheng, H.-L. You, X. Xu, Z.-M. Dong, An Early Cretaceous heterodontosaurid dinosaur with filamentous integumentary structures. *Nature* **458**, 333-336 (2009).
40. C. Chang, Y. Fang, S. Kinney, Climatic significance of quantitative analysis of rafted lithic debris with a focus on lake ice-rafted debris in the Junggar Basin, Xinjiang, NW China. *Geological Society of London Special Paper* **submitted** (2022).
41. P. Forster *et al.*, "The Earth's Energy Budget, Climate Feedbacks, and Climate Sensitivity" in *Climate Change 2021: The Physical Science Basis. Contribution of Working Group I to the Sixth Assessment Report of the Intergovernmental Panel on Climate Change*, V. Masson-Delmotte *et al.*, Eds. (Cambridge University Press, Cambridge, UK, 2021).

42. M. T. Jones, D. A. Jerram, H. H. Svensen, C. Grove, The effects of large igneous provinces on the global carbon and sulphur cycles. *Palaeogeography, Palaeoclimatology, Palaeoecology* **441**, 4–21 (2016).
43. M. R. Rampino, S. Self, Volcanic winter and accelerated glaciation following the Toba super-eruption. *Nature* **359**, 50-52 (1992).
44. M. Steinthorsdottir, A. J. Jeram, J. C. McElwain, Extremely elevated CO<sub>2</sub> concentrations at the Triassic/Jurassic boundary. *Palaeogeography, Palaeoclimatology, Palaeoecology* **308**, 418–432 (2011).
45. P. E. Olsen *et al.*, The Geological Orrery: Mapping the chaotic history of the Solar System using Earth's geological record. *SIAM Conference on Applications of Dynamical Systems, Snowbird, Utah* **DS19 - MS162-1**, [https://meetings.siam.org/sess/dsp\\_talk.cfm?p=98700](https://meetings.siam.org/sess/dsp_talk.cfm?p=98700); [https://www.pathlms.com/siam/courses/11697/sections/14920/video\\_presentations/129751](https://www.pathlms.com/siam/courses/11697/sections/14920/video_presentations/129751) (2019).
46. C. Elliott-Kingston, M. Haworth, J. C. McElwain, Damage structures in leaf epidermis and cuticle as an indicator of elevated atmospheric sulphur dioxide in early Mesozoic floras. *Review of Palaeobotany and Palynology* **208**, 25-42 (2014).
47. K. L. Bacon, B. C. M., M. Haworth, J. C. McElwain, Increased Atmospheric SO<sub>2</sub> Detected from Changes in Leaf Physiognomy across the Triassic–Jurassic Boundary Interval of East Greenland. *PLoS ONE* **8**, e60614 (2013).
48. A. R. Milner, J. I. Kirkland, The case for fishing dinosaurs at the St. George dinosaur discovery site at Johnson Farm. *Utah Geological Survey, Survey Notes* **39**, 1-3 (2007).
49. P. E. Olsen *et al.*, Mapping Solar System chaos with the Geological Orrery. *Proceedings of the National Academy of Sciences* **116**, 10664–10673 (2019).
50. J. Laskar, "Chapter 4 - Astrochronology" in *Geologic Time Scale 2020*, J. G. Ogg, M. D. Schmitz, G. M. Ogg, Eds. (Elsevier, Amsterdam, 2020), vol. 1, chap. 4, pp. 139-158.
51. L. J. Lourens, "The Variation of the Earth's Movements (Orbital, Tilt and Precession)" in *Climate Change: Observed Impacts on Planet Earth*, T. M. Letcher, Ed. (Elsevier, Amsterdam, 2015), pp. 399-418.
52. J. D. Hays, J. Imbrie, N. J. Shackleton, Variations in the Earth's orbit: Pacemaker of the Ice Ages. *Science* **194**, 1121-1132 (1976).
53. A. Strasser, F. J. Hilgen, P. H. Heckel, Cyclostratigraphy – concepts, definitions, and applications. *Newsletters on Stratigraphy* **42** (2006).
54. A. L. Berger, M. Loutre, Origine des fréquences des éléments astronomiques intervenant dans le calcul de l'insolation. *Bulletins de l'Académie Royale de Belgique* **1**, 45-106 (1990).
55. L. A. Hinnov, "Cyclostratigraphy and astrochronology in 2018" in *Cyclostratigraphy and Astrochronology*, M. Montenari, Ed. (Academic Press (Elsevier), London, 2018), pp. 1-80.
56. A. Douglass, P. E. Olsen, C. Chang, S. Kinney, B. B. Slibeck, Using Image Analysis and XRF to constrain orbital forcing and Climate in the Mediterranean Basin over the Last 500,000 Years. Using XRF Geochemistry. *Geological Society of America Abstracts with Programs* **54**, doi: 10.1130/abs/2022AM-382349, <https://gsa.confex.com/gsa/382022AM/meetingapp.cgi/Paper/382349> (2022).
57. S. R. Meyers, Cyclostratigraphy and the problem of astrochronologic testing. *Earth-science reviews* **190**, 190-223 (2019).
58. M. Li, L. Hinnov, L. Kump, Acycle: Time-series analysis software for paleoclimate research and education. *Computers & Geosciences* **127**, 12–22 (2019).
59. J. Laskar *et al.*, Long term evolution and chaotic diffusion of the insolation quantities of Mars. *Icarus* **170**, 343-364 (2004).
60. J. Laskar, A. Fienga, M. Gastineau, H. Manche, La2010: A new orbital solution for the long-term motion of the Earth. *Astronomy and Astrophysics* **532**, 1–15 (2011).
61. T. J. Blackburn *et al.*, Zircon U-Pb geochronology links the end-Triassic extinction with the Central Atlantic Magmatic Province. *Science* **340**, 941–945 (2013).

62. P. E. Olsen, M. S. Fedosh, Duration of the early Mesozoic extrusive igneous episode in eastern North America determined by use of Milankovitch-type lake level cycles. *Geological Society of America, Abstracts with Programs* **20**, 59 (1988).
63. P. E. Olsen, R. W. Schlische, P. J. W. Gore, Field Guide to the Tectonics, stratigraphy, sedimentology, and paleontology of the Newark Supergroup, eastern North America. *International Geological Congress, Guidebooks for Field Trips* **351**, 1-174 (1989).
64. P. E. Olsen, R. W. Schlische, M. S. Fedosh, "580 kyr duration of the Early Jurassic flood basalt event in eastern North America estimated using Milankovitch cyclostratigraphy" in *The Continental Jurassic*, M. Morales, Ed. (New Mexico Museum of Natural History and Science, Albuquerque, NM, 1996), pp. 11-22.
65. D. V. Kent *et al.*, Empirical evidence for stability of the 405-kiloyear Jupiter–Venus eccentricity cycle over hundreds of millions of years. *Proceedings of the National Academy of Sciences* **115**, 6153-6158 (2018).
66. R. A. Muller, G. J. MacDonald, *Ice ages and astronomical causes: data, spectral analysis and mechanisms* (Springer Science & Business Media, London, 2002).
67. R. A. Muller, G. J. MacDonald, Spectrum of 100-kyr glacial cycle: Orbital inclination, not eccentricity. *Proceedings of the National Academy of Sciences* **94**, 8329-8334 (1997).
68. R. T. Müller, M. S. Garcia, Oldest dinosauromorph from South America and the early radiation of dinosaur precursors in Gondwana. *Gondwana Research* **107**, 42-48 (2022).
69. P. Huybers, Combined obliquity and precession pacing of late Pleistocene deglaciations. *Nature* **480**, 229-232 (2011).
70. D. V. Kent, L. Tauxe, Corrected Late Triassic latitudes for continents adjacent to the North Atlantic. *Science* **307**, 240-244 (2005).
71. L. A. Hinnov, A. Cozzi, Rhaetian (Late Triassic) Milankovitch Cycles in the Tethyan Dachstein Limestone and Laurentian Passaic Formation Linked by the g2-g5 Astronomical Metronome. *Boletín Geológico y Minero* **131**, 269–290 (2020).
72. M. Margulis-Ohnuma, J. Whiteside, P. Olsen, Strong inclination pacing of climate in Late Triassic low latitudes revealed by the Earth-Saturn tilt cycle. *The Yale Undergraduate Research Journal* **2**, 1–9 (2021).
73. M. Rossignol-Strick, Mediterranean Quaternary sapropels, an immediate response of the African monsoon to variation of insolation. *Palaeogeography, Palaeoclimatology, Palaeoecology* **49**, 237-263 (1985).
74. M. Rossignol-Strick, African monsoons, an immediate climate response to orbital insolation. *Nature* **304**, 46-49 (1983).
75. L. J. Lourens *et al.*, Evaluation of the Plio - Pleistocene astronomical timescale. *Paleoceanography* **11**, 391-413 (1996).
76. S. Calvert, B. Nielsen, M. Fontugne, Evidence from nitrogen isotope ratios for enhanced productivity during formation of eastern Mediterranean sapropels. *Nature* **359**, 223-225 (1992).
77. T. F. Pedersen, S. E. Calvert, Anoxia vs. productivity: what controls the formation of organic-carbon-rich sediments and sedimentary rocks? *AAPG Bulletin* **74**, 454-466 (1990).
78. K. M. Grant *et al.*, The timing of Mediterranean sapropel deposition relative to insolation, sea-level and African monsoon changes. *Quaternary Science Reviews* **140**, 125-141 (2016).
79. M. J. Coolen, H. Cypionka, A. M. Sass, H. Sass, J. Overmann, Ongoing modification of Mediterranean Pleistocene sapropels mediated by prokaryotes. *Science* **296**, 2407-2410 (2002).
80. T. Konijnendijk, M. Ziegler, L. Lourens, Chronological constraints on Pleistocene sapropel depositions from high-resolution geochemical records of ODP Sites 967 and 968. *Newsl. Stratigr* **47**, 263-282 (2014).
81. L. J. Lourens, R. Wehausen, H. J. Brumsack, Geological constraints on tidal dissipation and dynamical ellipticity of the Earth over the past three million years. *Nature* **409**, 1029-1033 (2001).

82. A. Douglass, P. E. Olsen, C. Chang, S. Kinney, B. B. Slibeck, Scenes from the Sapropels: Revealing Orbital Forcings and Climate in the Mediterranean over the last 500 kyr with Image and XRF Analysis. *AGU Fall Meeting 2022 Abstract Submitted* (2022).
83. R. Hennekam *et al.*, Early - warning signals for marine anoxic events. *Geophysical Research Letters* **47**, e2020GL089183 (2020).
84. T. Sakamoto, T. Janecek, K.-C. Emeis (1998) Continuous sedimentary sequences from the eastern Mediterranean Sea: composite depth sections. in *Proceedings of the Ocean Drilling Program. Scientific results*, pp 37-59.
85. J. H. C. Bosmans, F. J. Hilgen, E. Tuenter, L. J. Lourens, Obliquity forcing of low-latitude climate. *Climates of the Past* **11**, 1335–1346 (2015).
86. J. H. C. Bosmans, S. S. Drijfhout, E. Tuenter, F. J. Hilgen, L. J. Lourens, Response of the North African summer monsoon to precession and obliquity forcings in the EC-Earth GCM. *Climate Dynamics* **44**, 279-297 (2015).
87. D. P. McInerney, J. F. Hubert, "Meandering-river facies in the upper Triassic New Haven Arkose, south central Connecticut: early evolution of the Hartford rift basin" in *The Great Rift Valleys of Pangea in Eastern North America*, P. M. LeTourneau, P. E. Olsen, Eds. (Columbia University Press, New York, 2003), vol. 2, Sedimentology, Stratigraphy, and Paleontology, pp. 88—107.
88. J. F. Hubert, A. A. Reed, W. L. Dowdall, J. M. Gilvhrst, *Guide to the redbeds of central Connecticut: 1978 field trip, Eastern Section of SEPM*, University of Massachusetts, Department of Geology and Geography, Contribution (Amherst, Massachusetts, 1978), vol. 32, pp. 129.
89. L. H. Gile, F. F. Peterson, R. B. Grossman, Morphological and genetic sequences of carbonate accumulation in desert soils. *Soil Science* **101**, 347-360 (1966).
90. Z. S. Wang, E. T. Rasbury, G. N. Hanson, W. J. Meyers, Using the U-Pb system of calcretes to date the time of sedimentation of clastic sedimentary rocks. *Geochimica et Cosmochimica Acta* **62**, 2823-2835 (1998).
91. P. E. Olsen, M. F. Schaller, D. V. Kent, Atmospheric CO<sub>2</sub> Amplification of Orbitally Forced Changes in the Hydrological Cycle in the Early Mesozoic. *AGU, 2015 Fall Meeting*, Paper PP53A-2321 (2015).
92. P. E. Olsen, H.-D. Sues, M. A. Norell, First record of *Erpetosuchus* (Reptilia: Archosauria) from the Late Triassic of North America. *Journal of Vertebrate Paleontology* **20**, 633-636 (2000).
93. D. Foffa *et al.*, Revision of *Erpetosuchus* (Archosauria: Pseudosuchia) and new erpetosuchid material from the Late Triassic 'Elgin Reptile' fauna based on  $\mu$ CT scanning techniques. *Earth and Environmental Science Transactions of the Royal Society of Edinburgh* **111**, 209–233 (2020).
94. A. R. Philpotts, A. Martello, Diabase feeder dikes for the Mesozoic basalts in southern New England. *American Journal of Science* **286** (1986).
95. P. E. Olsen, J. H. Whiteside, P. Huber, "Causes and consequences of the Triassic-Jurassic mass extinction as seen from the Hartford basin." in *Guidebook for Field Trips in the Five College Region, 95th New England Intercollegiate Geological Conference*, Department of Geology, Smith College, Northampton, Massachusetts, J. B. Brady, J. T. Cheney, Eds. (Smith College, Northampton, 2003), pp. B5-1 - B5-41.
96. T. M. Scheyer *et al.*, *Colobops*: a juvenile rhynchocephalian reptile (Lepidosauromorpha), not a diminutive archosauromorph with an unusually strong bite. *Royal Society Open Science* **7**, 192179 (2020).
97. H. D. Sues, D. Baird, A skull of a sphenodontian lepidosaur from the New Haven Arkose (Upper Triassic: Norian) of Connecticut. *Journal of Vertebrate Paleontology* **13**, 370–372 (1993).
98. A. C. Pritchard, J. A. Gauthier, M. Hanson, G. S. Bever, B. A. S. Bhullar, A tiny Triassic saurian from Connecticut and the early evolution of the diapsid feeding apparatus. *Nature communications* **9**, 1-10 (2018).
99. R. N. Greenberger *et al.*, Hydrothermal alteration and diagenesis of terrestrial lacustrine pillow basalts: Coordination of hyperspectral imaging with laboratory measurements. *Geochimica et Cosmochimica Acta* **171** (2015).

100. P. E. Olsen, D. V. Kent, M. Et-Touhami, Determining the concentration of individual eruptive events of the CAMP: Distinguishing interflow hiatuses from subterranean alteration and void infilling. *Geophysical Research Abstracts* **14**, EGU2012-13599 (2012).
101. Anonymous (2019) List of volcanic eruptions by death toll.
102. T. Thordarson, S. Self, The Laki (Skaftar Fires) and Grimsvotn eruptions in 1783-1785. *Bulletin of Volcanology* **55**, 233–263 (1993).
103. N. G. McDonald, *Window into the Jurassic world. Dinosaur State Park, Rockyr Hill, Connecticut.* ( Friends of Dinosaur State Park and Arboretum, Inc., Rockyr Hill, Connecticut, 2010), pp. 105.
104. J. B. Byrnes (1972) The Bedrock Geology of Dinosaur State Park, Rockyr Hill, Connecticut. (University of Connecticut, Storrs, Connnecticut), p 244.
105. B. Zangler, The Triassic rocks of Dinosaur State Park, Rockyr Hill, Connecticut. *Dinosaur State Park, Connecticut Geological and Natural History Survey*, 1-50 (1969).
106. P. A. Drzewiecki, T. Schroeder, R. P. Steinen, M. A. Thomas, The Bedrock Geology of the Hartford South Quadrangle: with a map and cross sections. *State Geological and Natural History Survey of Connecticut, Department of Energy and Environmental Protection, Quadrangle Report* **40** (2012).
107. G. Gierliński, The furry dinosaur. *Dinosaur World* **4**, 3–5 (1998).
108. M. G. Lockley, A. P. Hunt, P. Koroshetz, *Dinosaur Tracks: And other Fossil Footprints of the Western United States* (Columbia University Press, New York, 1999), pp. 360.
109. N. G. McDonald, P. M. LeTourneau, P. Huber, P. E. Olsen, "Early Jurassic lake-shoreline environments of the Hartford Basin: Fossils, food-chains, and implications for the facies-linked distribution of dinosaur tracks and track-makers" in *Dinosaur State Park*, J. O. Farlow, J. A. Hyatt, Eds. (Indiana University Press, Bloomington, Indiana, 2023).
110. C. Elton, *Animal Ecology* (Sudgwick & Jackson, London, 1927), pp. 96.
111. E. P. Odum, *Fundamentals of Ecology* (Saunders, Philadelphia, ed. 3rd, 1971), pp. 574.
112. P. E. Olsen, N. G. McDonald, "The stratigraphy and paleontology of the Newark Supergroup in its global context" in *Dinosaur State Park*, J. O. Farlow, J. A. Hyatt, Eds. (Indiana University Press, Bloomington, Indiana, 2023).
113. P. E. Olsen, "Paleontology and paleoenvironments of Early Jurassic age strata in the Walter Kidde Dinosaur Park (New Jersey, USA)" in *Field Guide and Proceedings of the Twelfth Annual Meeting of the Geological Association of New Jersey*, Geological Association of New Jersey, William Patterson College, Patterson, NJ., J. E. B. Baker, Ed. (William Patterson College, Paterson, NJ, 1995), pp. 156-190.
114. H.-D. Sues, P. E. Olsen, Stratigraphic and temporal context and faunal diversity of Permian-Jurassic continental tetrapod assemblages from the Fundy rift basin, eastern Canada. *Atlantic Geology* **51**, 139–205 (2015).
115. P. D. Krynine, *Petrology, stratigraphy, and origin of the Triassic sedimentary rocks of Connecticut*, State of Connecticut, State Geological and Natural History Survey, Bulletin (State of Connecticut, State Geological and Natural History Survey, Hartford, Connecticut, 1950), vol. 73.
116. G. D. Klein, "Trip C1: Sedimentology of Triassic Rocks in the lower Connecticut Valley" in *Guidebook for Fieldtrips in Connecticut*, New England Intercollegiate Geological Conference, 60th Annual Meeting, Yale University, New Haven, Connecticut, October 25-27, 1968, P. M. Orville, Ed. (State Geological and Natural History Survey of Connecticut, Guidebook, Hartford, Connecticut, 1968), chap. C-1, pp. C1–C19.
117. P. E. Olsen, A 40-million-year lake record of early Mesozoic orbital climatic forcing. *Science* **234**, 842–848 (1986).
118. N. H. Gray, "Mesozoic volcanism in north-central Connecticut" in *Guidebook for Field trips in Connecticut and South-Central Massachusetts*, R. Joesten, S. S. Quarrier, Eds. (1982), pp. 173–193.
119. A. Brignon, The earliest discoveries of articulated fossil fishes (Actinopterygii) in the United States: A historical perspective. *American Journal of Science* **317**, 216-250 (2017).

120. A. R. McCune, K. S. Thomson, P. E. Olsen, "Semionotid fishes from the Mesozoic Great Lakes of North America" in *Evolution of Species Flocks*, A. A. Echelle, I. Kornfield, Eds. (University of Maine at Orono Press, Orono, Maine, 1984), pp. 27-44.
121. N. G. McDonald, P. M. LeTourneau (1989) Taphonomic phosphate loss in Early Jurassic lacustrine fishes, East Berlin Formation, Hartford Basin, New England, USA. in *International Geological Congress, 28th Session, Washington, D.C., Abstracts* (, American Geophysical Union, Washington, DC), p 398.
122. E. Leonard (2013) The Taphonomy and Depositional Environment of Jurassic Lacustrine Fish Deposits, Westfield Bed, East Berlin Formation, Hartford Basin. in *Earth & Environmental Sciences* (Wesleyan University, Middletown, Connecticut), p 112.
123. P. M. LeTourneau, N. G. McDonald, P. E. Olsen, T. C. Ku, P. R. Getty, "Fossils and facies of the Connecticut Valley Lowland: Ecosystem structure and sedimentary dynamics along the footwall margin of an active rift" in *Guidebook for field trips in Connecticut and Adjacent regions: Middletown, Connecticut, Wesleyan University, New England Intercollegiate Geological Conference, 107th Annual Meeting, October 9–11, 2015. (Weslyan University, Middletown, Connecticut, 2015), vol. 9, pp. B2-1–B2-45.*
124. A. Meacham, Selective Preservation of Fossil Ghost Fish. *EGU General Assembly Conference Abstracts* **18**, 10524 (2016).
125. P. E. Olsen, "Tectonic, climatic, and biotic modulation of lacustrine ecosystems: examples from the Newark Supergroup of eastern North America" in *Lacustrine Basin Exploration: Case Studies and Modern Analogs*, B. Katz, Ed. (1990), pp. 209-224.
126. P. E. Olsen, S. Kinney, Early post-depositional bedding-plane-parallel melanges created by shear and liquefaction: A common but largely misinterpreted organic-rich mudrock facies. *Geological Society of America Abstracts with Programs* **48**, doi: 10.1130/abs/2016AM-287708 (2016).
127. K. M. Dyer-Pietras, Insolation forcing of sub-lacustrine debris flows – Could monsoon intensification have played a role? Eocene lacustrine Green River Formation, Piceance Creek Basin, Colorado. *Palaeogeography, Palaeoclimatology, Palaeoecology* **553**, 109738 (2020).
128. E. Gierlowski-Kordesch, P. Huber, "Trip B: Lake sequences of the central Hartford Basin, Newark Supergroup" in *Guidebook for Fieldtrips in Eastern Connecticut and the Hartford Basin, Northeastern Section, Geological Society of America, 30th Annual Meeting, Cromwell, Connecticut, March 19-22, 1995*, N. W. McHone, Ed. (State Geological and Natural History Survey of Connecticut, Hartford, Connecticut, 1995), vol. 7, pp. B1-B39.